Design, Modelling and Optimization of Solar Absorption Cooling System for Cold Storages in Pakistan

By

Musannif Shah

Reg # 00000204307

Session 2017-19

Supervised by

Dr. Adeel Javed

A Thesis Submitted to the US-Pakistan Center for Advanced Studies in Energy in partial fulfillment of the requirements for the degree of

MASTER of SCIENCE

in

THERMAL ENERGY ENGINEERING

US-Pakistan Center for Advanced Studies in Energy (USPCAS-E)

National University of Sciences and Technology (NUST)

H-12, Islamabad 44000, Pakistan

September 2020

THESIS ACCEPTANCE CERTIFICATE

Certified that final copy of MS/MPhil thesis written by Mr. Musannif Shah, (Registration No. 00000204307), of U.S. Pakistan Center for Advanced Studies in Energy has been vetted by undersigned, found complete in all respects as per NUST Statues/Regulations, is within the similarity indices limit and is accepted as partial fulfillment for the award of MS/MPhil degree. It is further certified that necessary amendments as pointed out by GEC members of the scholar have also been incorporated in the said thesis.

Signature: _____

Name of Supervisor: Dr. Adeel Javed

Date: _____

Signature (HoD): _____

Date: _____

Signature (Dean/Principal): _____

Date: _____

Certificate

This is to certify that work in this thesis has been carried out by **Mr. Musannif Shah** and completed under my supervision in, U.S. Pakistan Center for Advanced Studies in Energy (USPCAS-E), National University of Sciences and Technology, H-12, Islamabad, Pakistan.

Supervisor:

_____
Dr. Adeel Javed
USPCAS-E
NUST, Islamabad

GEC member # 1:

_____
Dr. Adeel Waqas
USPCAS-E
NUST, Islamabad

GEC member # 2:

_____
Dr. Majid Ali
USPCAS-E
NUST, Islamabad

GEC member # 3:

_____
Dr. Mariam Mahmood
USPCAS-E
NUST, Islamabad

HOD - Thermal Energy Engineering

_____
Dr. Adeel Javed
USPCAS-E
NUST, Islamabad

Principal/ Dean

_____
Dr. Adeel Waqas
USPCAS-E
NUST, Islamabad

Dedication

This thesis is dedicated specially to my dearest homeland; because of You I'm who I'm and I'm nothing without You.

And this also goes to my beloved father who was always there for me, my mother whose prays led me to this accomplishment, my adored siblings, without their tremendous support and cooperation it would never have been possible.

Lastly, this thesis is also dedicated to my friend Muhammad Shahzeb (late), who gave me the idea to join NUST to learn new things by acquiring challenging environment of study. May his soul rest in peace. Ameen

Acknowledgement

I would like to thank my Creator Allah Almighty, the Gracious, the beneficent, whose benediction bestowed upon me, provided me the ample opportunity and guided me throughout this work at every step.

I am grateful to my beloved parents who nurtured me and continued to support me throughout in every step of my life.

I would like to express special gratitude to my supervisor, Dr. Adeel Javed, for his guidance and support throughout this research. His advice and encouragement have been invaluable. Working on this project alongside him, I have grown professionally and have polished my research skills.

I would also like to thank the members of my GEC committee, Dr. Adeel Waqas, Dr. Mariam Mahmood and Dr. Majid Ali who honored my committee's presence. I would also acknowledge the facilities at USPCAS-E for providing me the software's to carry out comprehensive simulations involved in this work.

Finally, I am thankful to all the individuals who have rendered valuable assistance to my study.

Abstract

This study is focused on design and modelling of a novel solar assisted absorption cooling system for cold storage with banana facility located in Mardan, Pakistan. The system can be used to store up to 70,000 kg of banana in the temperature range of 14-16 ^{0}C. the system performance analysis is performed for two system configurations with a peak load of 82400 kJ/hr. (22.88kW). In configuration-1 (C-1), the fluid returning from the absorption chiller is always directed towards the stratified hot water storage tank which is connected to the evacuated tube solar thermal collectors. In configuration-2 (C-2), the fluid returning from the absorption chiller is diverted to absorption chiller instead of going towards the storage tank if its temperature is higher than the minimum operating temperature (e.g. 90 ^{0}C) of the absorption chiller. Both systems configurations were modelled in TRNSYS and simulations were carried out for whole year. Both configurations were optimized for lowest life cycle cost for 20 years by manipulating parameters (e.g. Solar collector area and Storage tank volume) affecting initial and operational cost of the system. Results reveals that C-2 have lowest life cycle cost 6.4 million PKR with optimum parameters of 120.3 m^2 collector area and 3.95 m^3 storage tank volume as compared to C-1 which have a life cycle cost of 28.4 million PKR for optimum parameters of 150 m^2 collector area and 1.98 m^3 storage tank volume.

Keywords: Cold storage, Solar absorption cooling, TRNSYS, Modelling, Optimization.

Table of Contents

List of Figures

List of Tables

List of Abbreviations and Symbols

Abbreviations

COP	Coefficient of performance
ETC	Evacuated tube collector
SAC	Solar absorption cooling
SCS	Solar cooling systems
SHC	Solar assisted heating and cooling system
TR	Tons of Refrigeration
TRNSYS	Transient system simulation
TMY	Typical meteorological year
VCR	Vapor compression refrigeration

Symbols

A_c	Area of Evacuated tube solar collector
a_o	Optical efficiency
a_1	Efficiency slope
a_2	Efficiency curvature
C_{pf}	Specific heat of the tank fluid
ε_{heat}	Boiler efficiency
$\dot{m}_h$	Fluid mass flow rate to tank from heat source
$\dot{m}_L$	Fluid mass rate to the load
T_{env}	Temperature of the environment surrounding the tank
$T_{g,i}$	Inlet temperature of the absorption chiller
$T_{g,o}$	Outlet temperature of the absorption chiller

$T_{col,o}$	Collector outlet temperature
$T_{st,o}$	Storage tank outlet temperature
$T_{ch,i}$	Chilled water inlet temperature
$T_{ch,o}$	Chilled water outlet temperature
$T_{cw,i}$	Cooling water inlet temperature
$T_{cw,o}$	Cooling water outlet temperature
T_{cs}	Conditioned space temperature
$\dot{Q_{solar}}$	Heat energy of the solar thermal collector
$\dot{Q_{boiler}}$	Heat energy of the auxiliary boiler
$\dot{Q_{hw}}$	Heat energy to the generator
$\dot{Q_{cw}}$	Heat energy rejected in the condenser
$\dot{Q_{ch}}$	Heat received from the evaporator

List of Publications

1. **Musannif Shah**, Adeel Javed, Hamid Ikram "Modeling and Optimization of Solar Absorption Cooling System for Cold Storages in Pakistan" in Proceedings of International Conference on Mechanical Engineering (ICME-2020)

Chapter 1: Introduction

1.1 Background

The agriculture sector contributes about 18.9 % in the GDP of Pakistan [1]. Banana is known as the premier fruit of Pakistan has a foremost effect on the agricultural economy of Pakistan. It is a leading fruit crop of Pakistan which is mainly cultivated in Sindh province due to its favorable soil and climatic condition for productive cultivation. The total portion of Sindh province in cultivation is 87%. It is cultivated on about 34,800 hectares area with a total production of 154,800 tons per year [2].

Due to the perishable nature of fruits and vegetables, industries associated with this business faces difficulties in postharvest management and marketing. Storage of fresh fruits and vegetables, after harvest, is one of the most pressing problems for tropical countries like Pakistan. Due to their high moisture content, vegetables and fruits are liable to spoil and have a very short life. Hence, preserving these types of fresh foods demands to be stored in controlled space e.g. temperature, humidity [3]. Cold storages are widely practiced methods for bulk handling of perishable fruits between production and marketing.

The banana facility is distinguished from other fruits by the process of ripening and requires conditions different from other fruits. Bananas must be green at the time of shipment to market to avoid injury during handling. Green bananas are held at 15°C, while temperatures below 14°C are to be avoided. When the bananas are to be ripened, the temperature is first brought up to about 25°C and maintained for some days until it ripens, and then brought back to 15°C and maintained for 3-5 days for the continuation of the storage. During the ripening process, the relative humidity level should be kept above 90% to keep it fresh [4].

Conventional cold storages for banana facilities use grid powered refrigeration system which are manufactured and installed by local consultants without proper engineering design and calculations. This inefficient system makes cold storage’s a major consumer

Figure 1.1: Conditioned space of a banana facility cold storage

Figure1.2: Conventional Refrigeration System

of energy among small scale commercial buildings. Fig 1 and 2 shows views of locally designed reference cold storage system.

Due to the non-availability of grid electricity in rural or remote locations and severe load shedding especially in summers, sellers are not able to achieve postharvest required conditions for banana storages which results in poor end quality and small storage period directly effecting end consumer. Hence, research is needed to find a new renewable energy solution for cold storage.

1.1.1 Pakistan Energy Scenario

Pakistan is facing a serious energy crisis and most of the less-developed areas are still not connected to the grid. The Energy supply and demand gap is huge and is widening over time. The country has very limited fossil fuel resources and needs to import, to fill this gap [5]. As a result of these power shortages, both urban and rural areas are experiencing significant load shedding [6]. Fig 3 shows the historical share of energy use in different sectors of Pakistan. It is clear from the statistics that the domestic and commercial sectors are the major consumers of energy [7]. In these sectors, electricity is widely used for air conditioning. Therefore, it is important to reduce the load from electricity by introducing other renewable energy sources for this purpose.

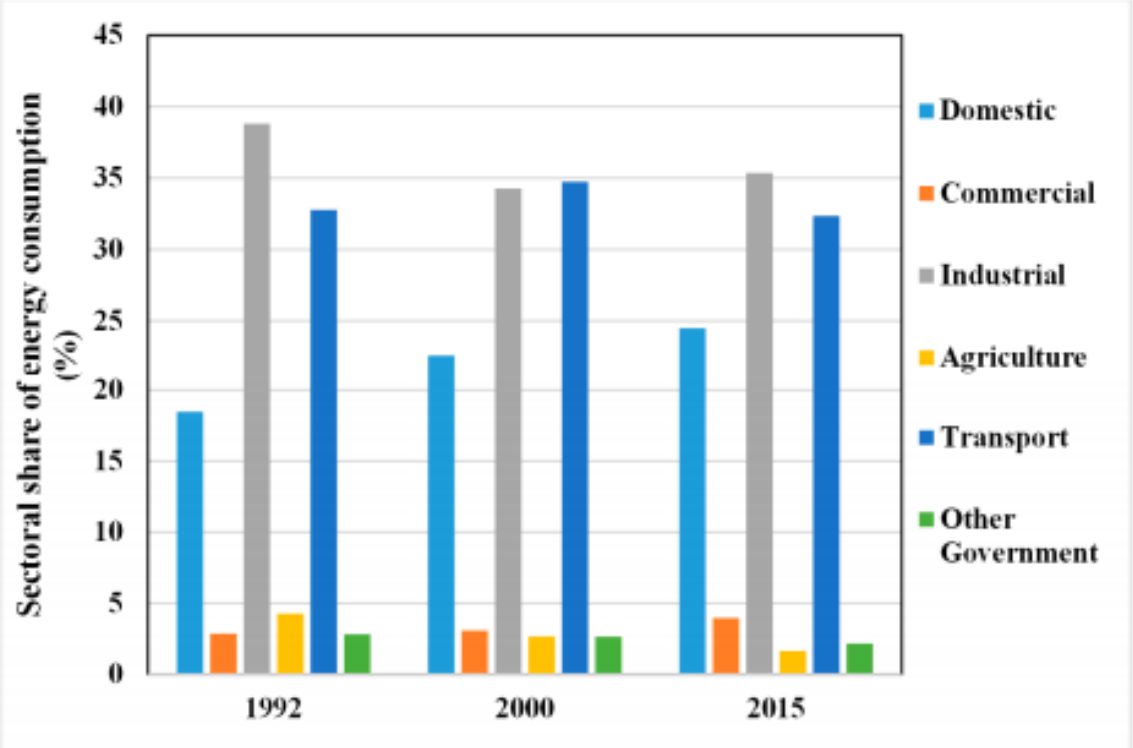

Figure 1.3: Historical share of energy consumption in different sectors

1.2 Conventional Cold Storage System

Most of the cold storages use vapor-compression refrigerators to achieve the required conditions. A refrigeration system mainly consists of three components; 1) The compressor, in which the refrigerant (mostly Ammonia) is compressed, 2) the condenser, either water-cooled or air-cooled, in which the hot gas from the compressor is cooled and condensed to liquid and 3) the evaporator cooling coils, in which the refrigerant is boiled by absorbing the heat from the storage room. Fans are installed for constant air circulation and better cooling [8]. These systems are very popular, due to their high coefficients of performance (COP), small size, and low weight as compared to other cooling systems. Currently, they use refrigerants: hydro-chlorofluorocarbon (HCFC) chloro-fluorocarbon (CFC) and hydro-fluorocarbons (HFC) [9]. The release of these refrigerants has contributed to the depletion of the ozone layer and has caused global warming since past 60 years [10]. One of the disadvantages of these systems is that these systems are very energy-intensive and require large investment of money to meet the demand for electricity[11].

Some facilities also use a vapor absorption refrigeration system, but it is cost-effective when there is an in-expensive source of low-temperature heat available[12]. The key design constraints for cold storage are uniformly maintaining the design temperature and relative humidity. Uniform temperature is maintained by adequate refrigeration capacity, the minimal temperature difference between the evaporator coil and the air temperature, uniform air distribution, and precise temperature control system.

1.3 Solar Cooling – An Attractive alternative

To mitigate environmental issues and to overcome the problems faced by conventional cooling systems, solar assisted absorption cooling system is of great interest [13][14]. These devices use thermal energy as an input to the refrigeration absorption cycle. The use of solar energy for cooling is an attractive option because the availability of resources is in line with the cooling load demand [15] Therefore, using these systems can reduce peak load demand of electricity and is appropriate to meet the cooling load requirements in buildings [16][17][18]. Thermally driven absorption refrigeration system utilizes environmentally friendly refrigerants such as; ammonia, methanol, and water, etc.

therefore they have no ozone depletion potential [9]. Additionally, the maintenance requirements of such a system are less because there are no rotating parts.

1.4 Advantages of Solar Cooling systems

Using solar absorption cooling system has the following advantages [19]

i. It reduces dependency on fossil fuels.
ii. By using such systems, the energy supply can be diversified.
iii. Have the potential to save limited natural reserves.
iv. Lessens CO_2 emissions.
v. The owner of such facilities can save money by reducing their bills.

1.5 Aims and Objectives

Overall, the comprehensive objective of this study is to model a solar thermal assisted absorption cooling system (SAC) for cold storage located in Mardan, Khyber Pakhtunkhwa, Pakistan (34.1989° N, 72.0231° E). Specifically, this project will aim on the following objectives.

i. Design and modeling of the SAC system for a banana facility using the Transient System simulation tool (TRNSYS).
ii. Performance analysis of the SAC system.
iii. Optimization of different components using the GenOpt optimization tool.
iv. Economic analysis of the system.

1.6 Motivation

The agricultural sector of Pakistan is contributing 18.9 % in the GDP, in which the banana facility is the main contributor. Existing fruit (banana) storages in Pakistan uses Vapor Compression based plant to attain conditioned space which are designed and installed by local consultants without proper calculations having excessive losses and highly inefficient setup causing more power consumption and extra billings. Also, Pakistan from the past decade is facing power crises and due to severe load shedding especially in the summer season [20] those fruit storages are unable to fulfill their cooling needs. Therefore, it is viable for Pakistan to use the SAC system for air-conditioning to reduce electricity load [21]. The motivation behind this project is to compute the cooling needs of fruit

storage and determine a new method for achieving the required cooling through hybrid solar thermal absorption cooling.

1.7 Scope of the work

In this study, a simulation model of a cold storage building is developed by using advanced building simulation software TRNBuild. The building selected for this study is a banana facility cold storage located in Mardan, Khyber Pakhtunkhwa Pakistan. The cooling load of the cold storage was estimated by considering, all the characteristics of the building (e.g. construction materials, internal heat gains, occupancy rate, etc.). Energy conservation measures (e.g. increasing insulation thickness) are applied to the building to investigate the reduction in the cooling load demand.

The performance of the SAC system for the actual cold storage building is observed by using TRNSYS 17 software. For modeling of the system, suitable components are selected from the TRNSYS library. Active cooling is achieved through hot water fired single effect Lithium Bromide (LiBr-H_2O) absorption chiller to accomplish the cooling needs of the cold storage. Other components included are evacuated tube collectors, a Stratified hot water storage tank, a closed-circuit cooling tower, auxiliary heater, pumps, and a fan. All these components are modeled in two different configurations C1 and C2. Both configurations are compared and optimized by total initial and operational cost for the coming 20 years using GenOpt tool.

1.8 Study limitations

This study is only limited for cold storages having a banana facility, because the cooling load is specifically calculated for the banana facility. For other cold storages such as; apple storages, dry fruit storages, and frozen storages the required temperature would change. Therefore, the cooling load and the size of the SAC system will also change.

Optimization and economic analysis of single effect LiBr-H_2O absorption chiller is performed in this study. Hence, this study is not valid for double-effect absorption chiller as the operational conditions and parameters are different for double-effect absorption chillers.

The experimental setup of the solar absorption cooling system for cold storage building is not developed because of the high capital cost of equipment and installation of the system.

1.9 References

[1] H. Census, M. Kharif, T. Fishing, K. Pakhtunkhwa, O.- December, and A.- May, "Chapter 2," 2017.

[2] C. E. O. Sedf, "A TECHNICAL GUIDE BOOK OF BANANA PREPARED AND COMPILED BY SUPERVISED BY," pp. 1–66.

[3] A. Basediya, D. V. K. Samuel, and V. Beera, "Evaporative cooling system for storage of fruits and vegetables - a review," vol. 50, no. June, pp. 429–442, 2013, doi: 10.1007/s13197-011-0311-6.

[4] A. S. Distinguished, F. Comfort, and A. I. R. Conditioning, "THE FIELD OF INDUSTRIAL."

[5] T. Muneer, S. Maubleu, and M. Asif, "Prospects of solar water heating for textile industry in Pakistan," vol. 10, pp. 1–23, 2006, doi: 10.1016/j.rser.2004.07.003.

[6] M. Farooq and A. Shakoor, "Severe energy crises and solar thermal energy as a viable option for Pakistan," vol. 013104, pp. 1–12, 2013.

[7] S. Aziz *et al.*, "The Future of Sustainable Energy Production in Estimating Hubbert Peaks," doi: 10.3390/en10111858.

[8] "raghavan1985.pdf." .

[9] K. Habib, B. Choudhury, P. Kumar, and B. Baran, "Study on a solar heat driven dual-mode adsorption chiller," *Energy*, vol. 63, pp. 133–141, 2013, doi: 10.1016/j.energy.2013.10.001.

[10] J. P. Praene, O. Marc, F. Lucas, and F. Miranville, "Simulation and experimental investigation of solar absorption cooling system in Reunion Island," *Appl. Energy*, vol. 88, no. 3, pp. 831–839, 2011, doi: 10.1016/j.apenergy.2010.09.016.

[11] A. M. Papadopoulos, S. Oxizidis, and N. Kyriakis, "Perspectives of solar cooling in view of the developments in the air-conditioning sector," vol. 7, pp. 419–438, 2003, doi: 10.1016/S1364-0321(03)00063-7.

[12] "The Commercial Storage of Fruits, Vegetables, and Florist and Nursery Stocks," no. 66, 2016.

[13] F. Palacín, C. Monné, and S. Alonso, "Improvement of an existing solar powered absorption cooling system by means of dynamic simulation and experimental diagnosis," *Energy*, vol. 36, no. 7, pp. 4109–4118, 2011, doi:

10.1016/j.energy.2011.04.035.

[14] C. Monné, S. Alonso, F. Palacín, and L. Serra, “Monitoring and simulation of an existing solar powered absorption cooling system in Zaragoza (Spain),” *Appl. Therm. Eng.*, vol. 31, no. 1, pp. 28–35, 2011, doi: 10.1016/j.applthermaleng.2010.08.002.

[15] X. Q. Zhai, R. Z. Wang, J. Y. Wu, Y. J. Dai, and Q. Ma, “APPLIED Design and performance of a solar-powered air-conditioning system in a green building,” vol. 85, pp. 297–311, 2008, doi: 10.1016/j.apenergy.2007.07.016.

[16] C. Sanjuan, S. Soutullo, and M. R. Heras, “Optimization of a solar cooling system with interior energy storage,” *Sol. Energy*, vol. 84, no. 7, pp. 1244–1254, 2010, doi: 10.1016/j.solener.2010.04.001.

[17] X. Q. Zhai, M. Qu, Y. Li, and R. Z. Wang, “A review for research and new design options of solar absorption cooling systems,” vol. 15, pp. 4416–4423, 2011, doi: 10.1016/j.rser.2011.06.016.

[18] X. Garcı, “Solar absorption cooling in Spain : Perspectives and outcomes from the simulation of recent installations ´ a Casals *,” vol. 31, pp. 1371–1389, 2006, doi: 10.1016/j.renene.2005.07.002.

[19] R. Article, “REVIEW OF SOLAR ABSORPTION REFRIGERATION SYSTEM USING LiBr-WATER AND SIMULATE THE Address for Correspondence,” vol. II, no. Ii, 2013.

[20] F. Jamil and E. Ahmad, “The relationship between electricity consumption , electricity prices and GDP in Pakistan,” *Energy Policy*, vol. 38, no. 10, pp. 6016–6025, 2010, doi: 10.1016/j.enpol.2010.05.057.

[21] A. Gastli and Y. Charabi, “Solar water heating initiative in Oman energy saving and carbon credits,” *Renew. Sustain. Energy Rev.*, vol. 15, no. 4, pp. 1851–1856, 2011, doi: 10.1016/j.rser.2010.12.015.

Chapter 2: Literature Review

2.1 Overview

Numerous studies are carried out to study different solar cooling techniques for buildings. Solar cooling can be achieved by integrating solar PV or solar thermal collectors with cooling generation systems. The efficiency of solar thermal collectors increases as the ambient temperature increases whereas, for solar PV modules, the efficiency reduces. Hence for hot climates like Pakistan, solar thermal cooling (e.g. solar absorption system) is more feasible than solar electric cooling[1], [2]. Several studies report the use of absorption refrigeration systems for cooling, using TRNSYS simulation software.

Tao He et. al. [3] modeled a solar absorption cooling system for a typical office building in Beijing, China using TRNSYS software. The cooling load of the office building was 50 TR. Evacuated tube solar thermal collectors with an aperture area and a tilt angle of 10^0 facing south were used. The rated capacity and COP of the absorption chiller was 175.8 kW and 0.7 respectively. A biomass boiler is also installed as a backup energy source. The optimum volume of cooling and heat storage tanks are 8 m^3 and 15 m^3 respectively. The of solar thermal collector's average annual efficiency was found to be 37.6% and the solar fractions calculated for both winters and summers were 0.38 and 0.76 respectively. Also, the coefficient of performance (COP) of the system for the whole summer season was found to be 0.32.

Tsoutsos et. al. [4] studied the performance evaluation of solar cooling and heating system for a hospital in Crete, Greece using TRNSYS. Different parameters like solar collector area and slope, storage tank volume, backup heater capacity, size of the cooling tower, and the absorption chiller nominal capacity were optimized. Four different situations were analyzed based on solar fraction and it was inferred that the optimum area for collector was 500 m^2 and the total optimum number of thermal collectors were 179. The solar fraction for cooling and heating season found were 74.24 % and 70.78 % respectively.

Florides et. al. [5] modeled and simulated a domestic size solar absorption cooling system using TRNSYS. The system consisted of compound parabolic collectors, a storage tank, a boiler, and a LiBr-water absorption chiller. Optimization revealed that 15 m^2 collector area tilted at 30^0 from horizontal and a hot storage tank with 600 L volume will run the

system at optimum conditions. The economic analysis concluded that the total life cycle cost of the system, for a lifetime of 20 years will be C£ 13,380 in which the cost of the absorption cooling system alone was found to be C£ 4800. The results also concluded that for an absorption system to be economically feasible as compared to a conventional cooling system its capital cost should be below C£ 2000.

Molero et. al. [6] compared two different models for SAC system for a residential building in Spain. Different parameters like solar collector area, COP, and setpoint temperature of absorption chiller and volume of thermal storage were optimized. The main objective of this study was to define the effects of hot and cold storage tanks. It was concluded from the results that the absorption cooling system performs better when a cold storage tank is used, especially when for larger storage size and smaller collector area.

Muhammad et. al. [7] did a simulation-based study of solar absorption cooling system for an educational building located at Islamabad. Various performance parameters such as solar fraction, solar collector efficiency, and primary energy savings were analyzed for two different configurations using TRNSYS to optimize system design variables like type and size of the collector, collector tilt angle, and storage tank volume. Results revealed that the second configuration having a flow diverter installed after the absorption chiller has higher primary energy savings irrespective of the collector type being used.

A multi-objective optimization study was carried out for a medium-sized office building located at four different locations (e.g. Phoenix, Atlanta, Los Angeles, Chicago) to investigate the performance parameters of a solar assisted absorption cooling and heating system by incorporating simultaneously different parameters like economic, environmental and energy aspects. The proposed method of analysis included central composite design, regression, and multi-objective optimization. The results suggested that the above approach can provide a systematic mechanism to design a solar assisted absorption cooling and heating system [8].

Yunlong et. al. [9] investigated the feasibility analysis of three different types of solar assisted air conditioning systems (e.g. solar desiccant-evaporative cooling system, solar desiccant-compression cooling system, solar absorption cooling system) for a typical office building for eight different cities of Australia. The technical and economic performance of each system was evaluated based on a solar fraction, COP, annual

electricity consumption, annual CO_2 emission reductions, and payback period. Results revealed that solar absorption cooling (SAC) system and solar desiccant evaporative (SDEC) systems are both energy-efficient systems but SDEC's were concluded as the most economically feasible solution for most of the Australian cities.

Ehsan et. al. [10] studied the improvement of the overall energy performance (e.g. retrofit cost, energy savings, and thermal comfort) of an existing residential building by retrofitting strategies. In their study, they developed a simulation-based multi-objective optimization model using TRNSYS, GenOpt, and MATLAB. In the analysis, they considered different materials for external walls and roof insulations, different types of windows and have installed solar collectors in the existing building. The results of the study verify the practicability of the approach and highlight the problems which may arise.

Al-Alili et. al. [11] studied both single-objective and multiple-objective optimization of the 10-kW solar assisted absorption system for Abu Dhabi's weather conditions. In the single-objective technique, the system performance and initial cost were optimized separately. Results reveal that the global minimum heater consumption was 1845 kW h, and the global minimum total cost, for a solar fraction of 0.5, was $72,203. Whereas in multi-objective technique, when the system performance and cost were optimized simultaneously, revealed that there were heater consumption reduction and cost savings up to 35.3% and 24.5% respectively.

2.2 Refrigeration

Refrigeration is a thermodynamic cycle which removes heat from the low temperature reservoir and rejects it to the high temperature reservoir. This cycle requires work as an input so that the second law of thermodynamics is not violated. The systems used for refrigeration are also called as cooling or air conditioning systems [12].

2.2.1 Various Methods for Refrigeration

There are two major methods of refrigeration which are,

1. Vapor Compression system
2. Vapor Absorption system

2.2.1.1 Vapor Compression System

It is the most widely used refrigeration cycle. The vapor compression refrigeration cycle consists of four components: Compressor, Condenser, Expansion valve, and Evaporator. The ideal vapor compression cycle mainly consists of four processes.

1-2 Isentropic compression process in the Compressor

2-3 Heat rejection process at constant pressure in the Condenser

3-4 Throttling process in the Expansion valve

4-1 Heat Absorption process at constant pressure in the Evaporator

In an ideal vapor-compression refrigeration cycle, the refrigerant first enters the compressor as a saturated vapor at state 1, where the temperature and pressure of the refrigerant are increased well above from the ambient conditions. The refrigerant then enters the condenser at state 2, where heat is rejected at constant pressure to the surrounding, and its temperature decreases to state 3. The saturated liquid refrigerant then enters an expansion device where the throttling process occurs, and the pressure decreases to evaporator pressure. The temperature after the expansion process drops well below the conditioned space temperature. The refrigerant then absorbs heat from the conditioned space and vaporizes and reenter as a saturated vapor to the compressor, completing the cycle [13]. The complete cycle is shown in figure 2.1.

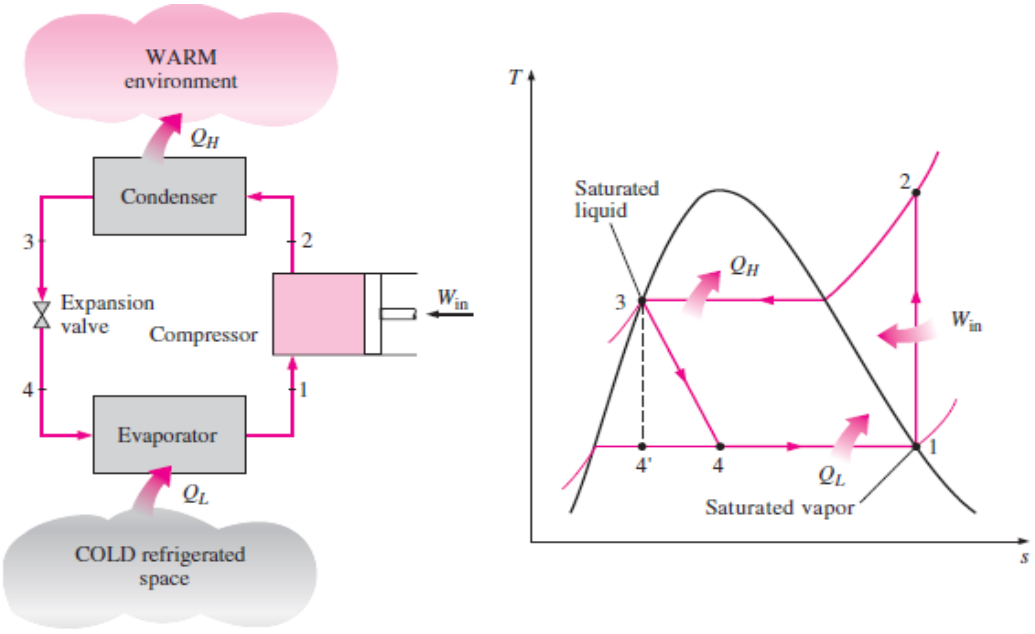

Figure 2.1: Schematic and T-s diagram for ideal vapor compression refrigeration cycle [13]

2.2.1.2 Vapor Absorption system

As the name implies, the absorption refrigeration cycle involves the absorption of refrigerant through a transport medium. The absorption system is one of the oldest refrigeration technologies. These systems operate on heat energy as an input, unlike vapor compression refrigeration. Moreover, they do not require compressors for the compression of refrigerants therefore, they require less maintenance. This form of refrigeration becomes economically attractive when there is an inexpensive thermal

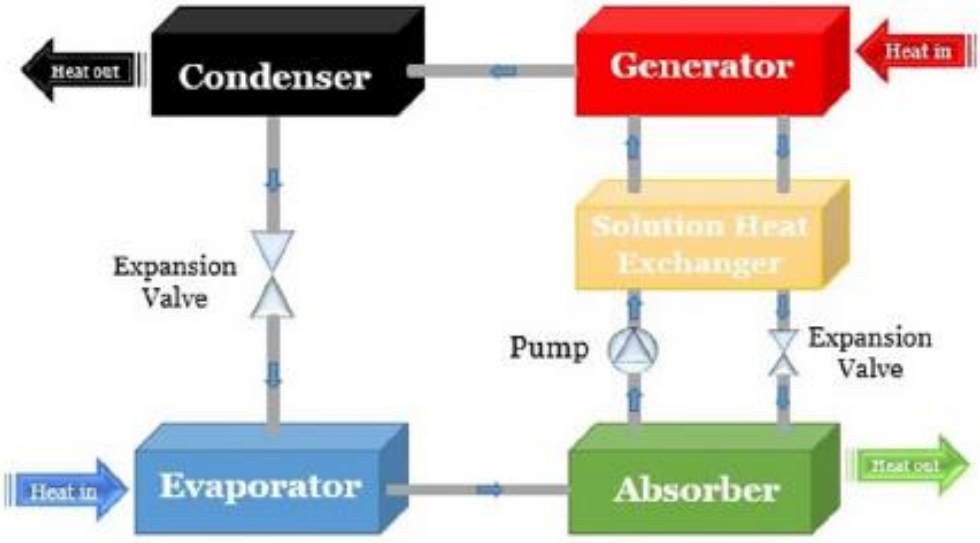

Figure 2.2: General Schematic diagram of vapor absorption system [14]

energy source at a temperature 100 to 200 ^{o} C (i.e. Solar energy, Geothermal energy, waste heat from powerplants and natural gas etc.) available. As Shown in the figure 2.2, an absorption refrigeration system has four main components: Generator, Condenser, Evaporator and Absorber [14].

2.2.1.3 Types of vapor absorption refrigeration systems

The improvement of the absorption system performance is done by development of the cycle design.[14]

a) Single Effect Absorption Cycle

- It has only one Generator to generate refrigerant (Figure 2.3)
- The COP of the system ranges between 0.35 to 0.7 (Figure 2.6)
- The generator temperature required is between 70 to 115 ^{0} C

- Low Cost as compared to multi effect

b) Double Effect Absorption Cycle

- It has two generators (i.e. High temperature generator (HTG) and low temperature generator (LTG)) (Figure 2.4)
- The COP of the system ranges between 0.8 to 1.3 (Figure 2.6)
- The generator temperature required is between 115 to 190 ^{0} C

c) Triple Effect Absorption Cycle

- It has three generators (i.e. Low temperature generator (LTG), Middle temperature generator (MTG) and High temperature generator (HTG)) (Figure 2.5)
- The COP of the system ranges between 1.1 to 1.8 (Figure 2.6)
- The generator temperature required is between 135 to 225 ^{0} C

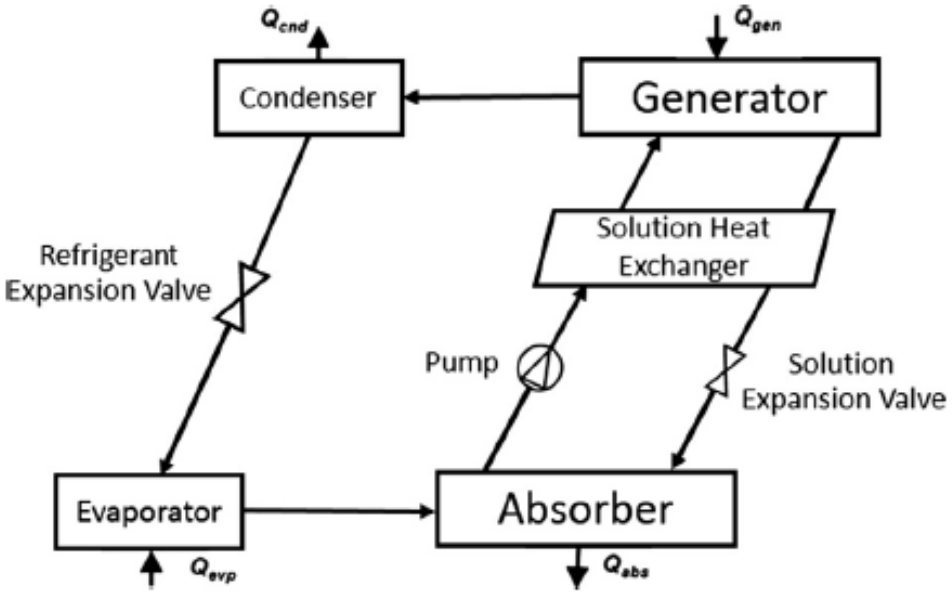

Figure 2.3: Schematic diagram of single-effect absorption refrigeration system [14]

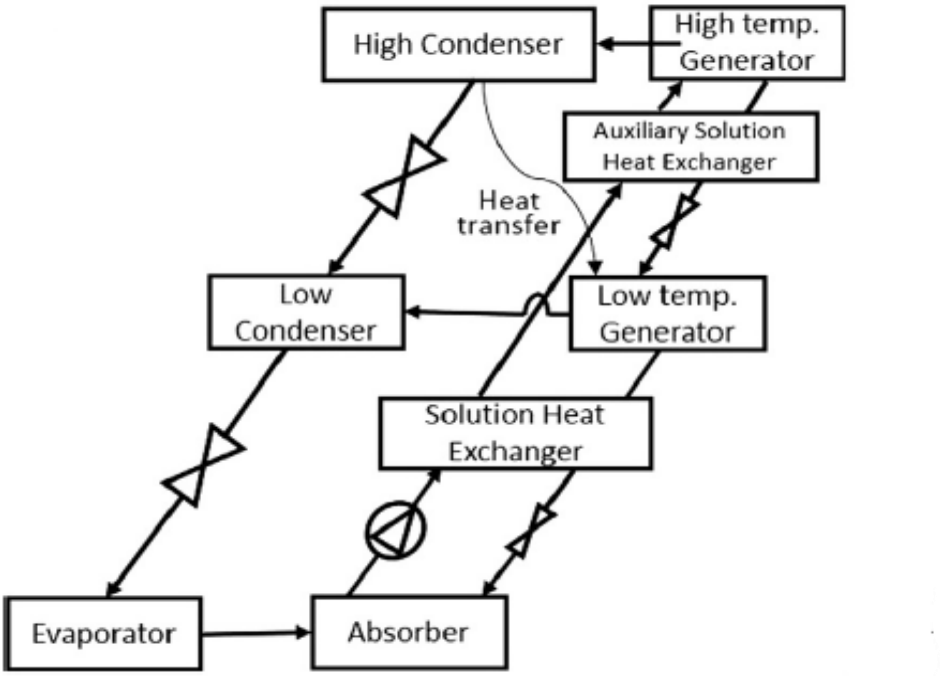

Figure 2.4: Schematic diagram of double-effect absorption refrigeration system [14]

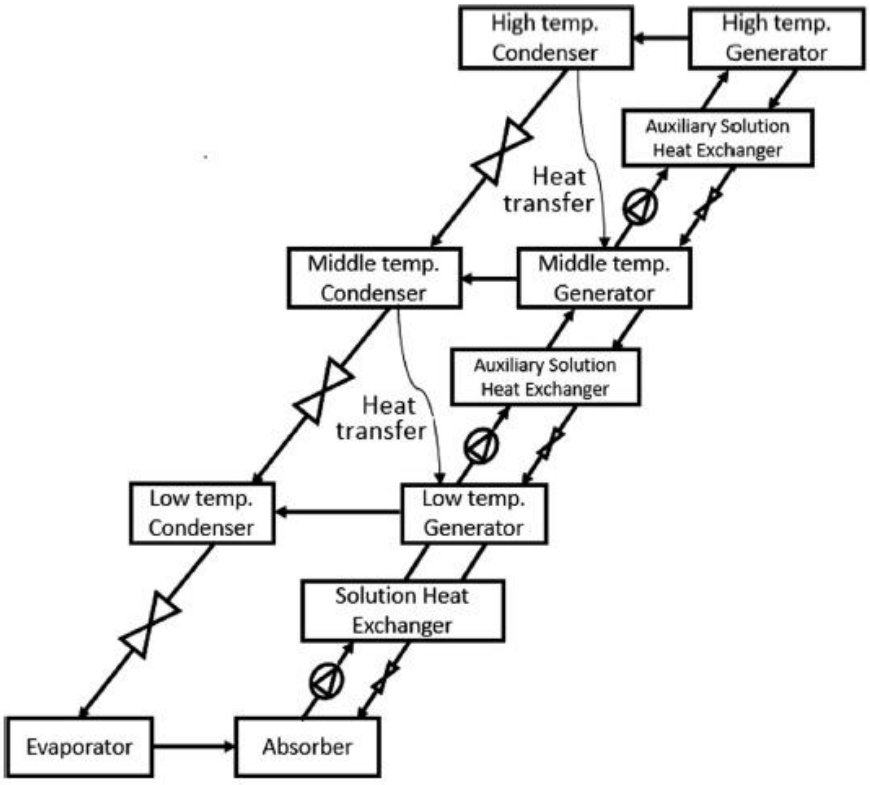

Figure 2.5: Schematic diagram of triple-effect absorption refrigeration system [14]

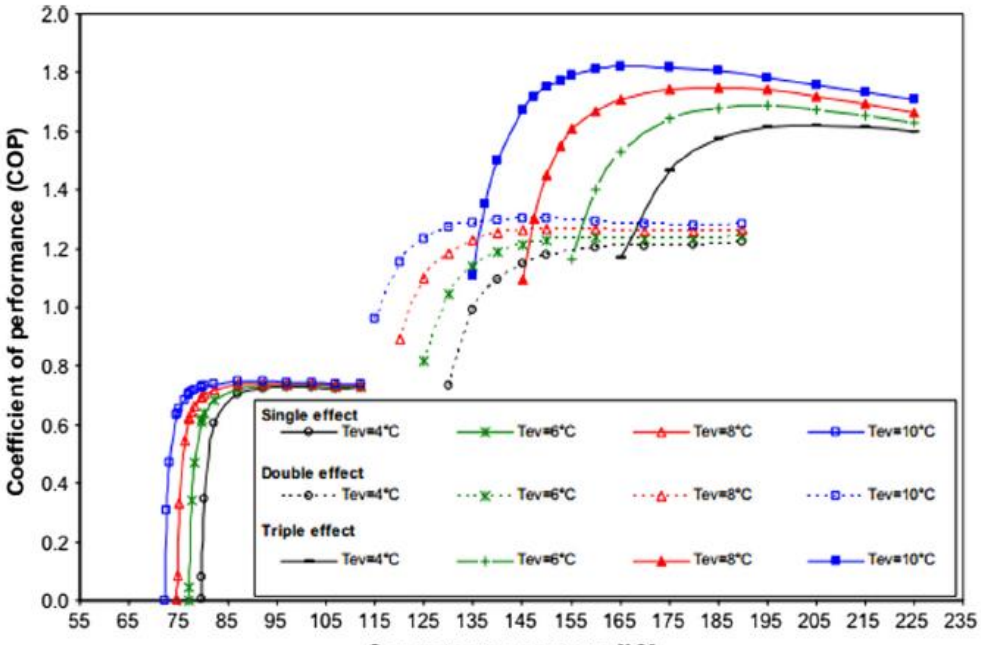

Figure 2.6: Variation of COP for single, double and triple effect absorption refrigeration system with generator temperature [14]

2.2.1.4 Refrigerant – Absorbent pairs

An appropriate pair of absorbent and refrigerant is of great importance in vapor absorption refrigeration system because the efficiency of the system is greatly influenced by the thermodynamic properties of the solution. The most familiar pairs are given below [5].

- Lithium Bromide (LiBr) – Water (H_2O) pair.

  This pair is more suitable for large scale solar based commercial applications because the temperature required for the generator is between 90 and 120 ^{0} C

- Ammonia (NH_3) – Water (H_2O) pair.

  This pair is frequently used for small scale residential and commercial applications. The temperature required for generator is between 125 and 170 ^{0} C.

2.2.1.5 Advantages of Absorption refrigeration system [14]

- Vapor absorption refrigeration system can be driven by a low-grade heat source (e.g. waste heat, solar energy etc.) which makes this system very effective in reducing CO_2 emissions.
- Vapor absorption refrigeration systems uses environment friendly refrigerants such as water, hence causing no effect on ozone layer and global warming.
- These systems mostly operate quietly as they have almost no high-speed moving parts. This also makes their maintenance cheaper and easier.

- Using absorption systems offer heat recovery from almost any system.
- There is no cycling loss during on-off operation in using vapor absorption refrigeration system.
- Vapor absorption refrigeration systems are considered durable with an expected lifetime of 20 to 30 years.

2.3 Solar Cooling Systems

2.3.1 Solar Electric Vapor Compression Refrigeration System

A solar electric refrigeration system mainly consists of photo-voltaic panels and refrigeration device. The input energy required to run the compressor of vapor compression system is provided by solar PV array as shown in the figure 2.7. the solar system always comes up with hybrid technology, because if the energy requirement of the system is not met by PV system the electricity is then supplied from the grid and the extra power from the PV is stored in the batteries. As can be seen from the figure 2.7 most of the system equipment's are AC based, Therefore, an inverter is also installed after PV array. This technology is cost, and energy saving and have less harmful effects on the environment [15].

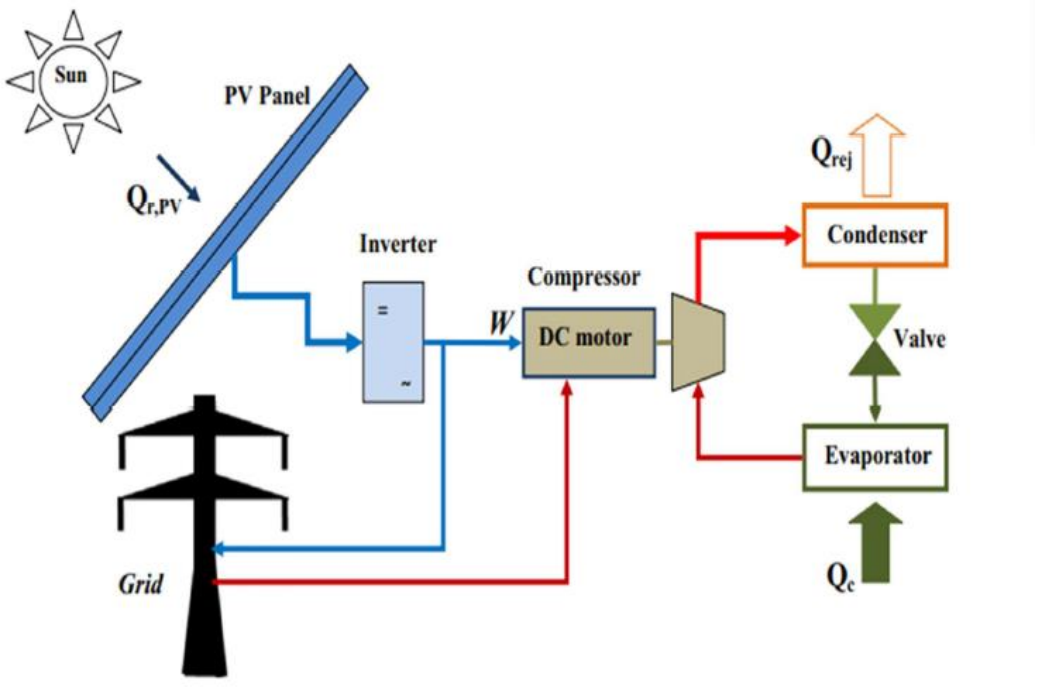

Figure 2.7: Schematic diagram of solar electric vapor compression refrigeration system [15]

2.3.2 Single Effect Solar Absorption Refrigeration System

Absorption refrigeration system requires heat energy as an input to the generator of the absorption chiller to produce water vapor from Lithium Bromide (LiBr) and Water (H_2O) solution. The heat energy required for the cycle can be supplied by industrial waste heat, solar collectors, boilers etc. Figure 2.8 shows working principle of solar collector-based vapor absorption system (SAC). In solar cooling, solar collectors harvest useful energy from the sun. The heat from the collector is used to heat working fluid (e.g. water) which is then stored in a storage tank. This hot water from the storage tank flows into the generator of the absorption chiller, where it is used to produce water vapor from LiBr-H_2O solution. In the generator pressurized water vapors at high temperature are formed. The pressurized water vapors are then passed through condenser where it rejects heat to the surrounding and is converted into liquid. After passing through the expansion device the low-pressure liquid water then passes through evaporator where it absorbs heat from the conditioned space.

In the meantime, strong solution from the generator returns to the absorber by passing through a regenerator where it pre heats the weak solution of LiBr-H_2O. Water vapors leaving the evaporator enters the absorber where it is mixed with strong solution of LiBr-H_2O [13]. For continues supply of the input hot water, an auxiliary heater is also installed.

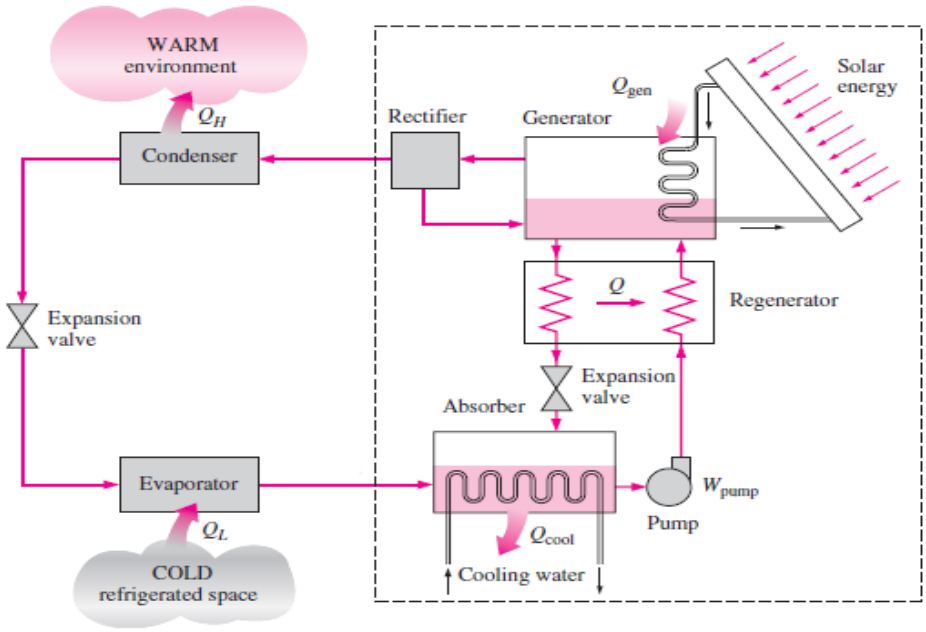

Figure 2.8: Schematic diagram for solar vapor absorption refrigeration cycle [13]

Whenever sufficient solar energy is not available the auxiliary heater heats the water to the required level. [16].

2.3.2.1 Process Description

The main steps in a single effect absorption cooling process are presented in Pressure Vs Temperature chart as shown in figure 2.9 [16]

1) The line 1-7 illustrates the pumping process of the weak solution from the absorber at point 1 to the generator at point 7 by passing through a heat exchanger. Whereas the concentration of the solution during process 1-7 remains the same.
2) The line 7-2 shows the sensible heating of the weak solution by hot water in the generator. The process is sensible heating only because only the temperature of the weak solution rises. The line 2-3 shows the latent heating process of the solution, which results in boiling of water in the condenser at constant pressure. During this heating step, water vapors evaporates from the solution which changes the weak solution into strong solution.
3) Path 3-8 indicates a process when the strong solution moves from the generator to the absorber through the heat exchanger. The energy from the strong solution is utilized to pre heat the weak solution coming from the absorber to the generator. During this process lithium Bromide (LiBr) concentration remains the same.

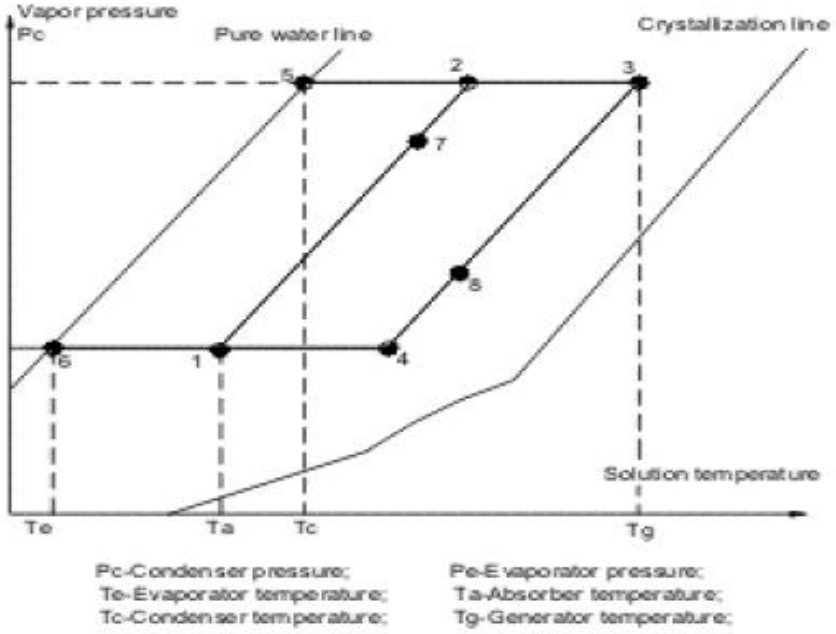

Figure 2.9: Process diagram of single effect absorption refrigeration cycle [16]

4) Process 8-4-1 shows an ideal process of absorption of water vapor from the evaporator by the strong solution present in the absorber.
5) During process 2-5 the water vapors rejects heat at constant pressure to the surroundings.
6) The water condenses after rejecting heat in the cooling towers. The condensed water then flows towards the evaporated indicated by line 5-6
7) In process 6-1 heat is absorbed from the conditioned space at constant pressure which causes the water in the evaporator to evaporate. The water vapor is then absorbed by the strong solution in the absorber completing the cycle.

2.4 Solar Thermal Collectors

Solar thermal collectors are heat exchanging devices that absorbs solar radiation from the sun and transform it into internal energy of the working fluid (e.g. air or water). The harvested solar energy is then carried away by circulating fluid either directly to the equipment for heat transfer or to the thermal energy storage for later use [17].

Generally solar thermal collectors are divided into two main types: a) Concentrating collectors b) Non-concentrating collectors. Non concentrating collectors are relatively cheaper than concentrating solar collectors, but it can only provide heated water which could only be used for less efficient single effect absorption refrigeration system. [18], [19]. The non-concentrating collectors which are available in Pakistan are:

1. Flat Plate Solar Collectors
2. Evacuated Tube Solar Collectors

Flat plate collectors (FPC) are the most common type of collectors used in the world [20]. It has a metallic absorber surface which absorbs solar radiations. There is an anti-reflective coating with glass plate installed on the surface of the FPC which reduces the reflective losses from the surface of the collector[21]. Evacuated tube collectors (ETC) are made from evacuated glass tubes which contains metallic absorber inside. ETC have less heat loss and they perform better at high temperatures. The schematic diagrams of both types of collectors is shown in the figure 2.10.

A solar thermal collector provides heat to the thermally operated refrigeration system. The efficiency of a solar thermal collector primarily depends upon the working temperature of the collector. At high working temperatures, due to higher temperature difference between the collector's working temperature and ambient temperature, the collector losses more

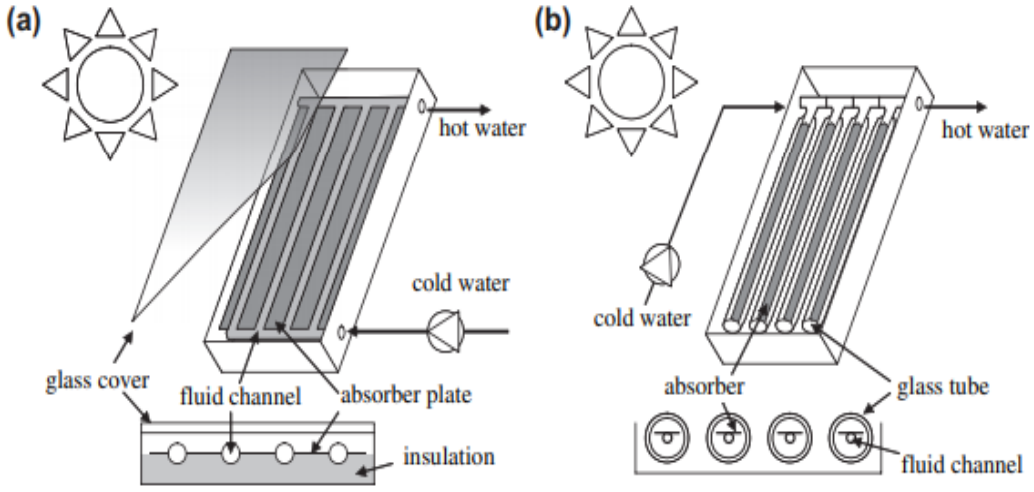

Figure 2.10: Schematic diagrams of solar collectors a) Flat plate type b) Evacuated tube type

heat and delivers less heat. Conversely, thermal refrigeration systems generally work more efficiently with a higher temperature input. While designing a solar thermal system, these two opposite trends must be considered [23].

2.5 Introduction to TRNSYS

TRaNsient SYstem Simulation (TRNSYS) is extensively used, thermal dynamic process simulation program. It was first developed for solar energy applications and simulations, now it can also be used for a wider variety of thermal processes [24]. TRNSYS can be used for Solar thermal heating and cooling, Solar PV and Building energy analysis. System components from the TRNSYS library can be interconnected in any manner. The OUTPUT from any component can be used as an INPUT to other components [25]. Each component in the TRNSYS library has a unique TYPE number (e.g. Type 1 is the solar collector, Type 56 is used for multi zoned building model). The components in TRNSYS library includes Solar collectors, thermostats, absorption chiller, hot water storage tanks, heat pumps, fans and many more. Literature shows that TRNSYS can provide less than 10% error between simulation results and actual operating system.

TRNSYS consists of many programs. This study only uses simulation studio. TRNSYS simulation software is centered on well-established analytical and empirical correlations which makes it a mature simulation tool. This software is being used to predict the long-term performance of a simulation system in the designing phase. The aim of current study is to design, model and recommend a solar based cooling system for a local Banana cold storage in Pakistan. For which TRNSYS software is used to model and simulate various design concepts and methods which were previously not considered and analyzed.

2.6 References

[1] K. R. Ullah, R. Saidur, H. W. Ping, R. K. Akikur, and N. H. Shuvo, "A review of solar thermal refrigeration and cooling methods," *Renew. Sustain. Energy Rev.*, vol. 24, pp. 499–513, 2013, doi: 10.1016/j.rser.2013.03.024.

[2] T. Otanicar, R. A. Taylor, and P. E. Phelan, "Prospects for solar cooling - An economic and environmental assessment," *Sol. Energy*, vol. 86, no. 5, pp. 1287–1299, 2012, doi: 10.1016/j.solener.2012.01.020.

[3] T. He *et al.*, "Application of Solar Thermal Cooling System Driven by Low Temperature Heat Source in China," *Energy Procedia*, vol. 70, pp. 454–461, 2015, doi: 10.1016/j.egypro.2015.02.147.

[4] T. Tsoutsos, E. Aloumpi, Z. Gkouskos, and M. Karagiorgas, "Design of a solar absorption cooling system in a Greek hospital," *Energy Build.*, vol. 42, no. 2, pp. 265–272, 2010, doi: 10.1016/j.enbuild.2009.09.002.

[5] G. A. Florides, S. A. Kalogirou, S. A. Tassou, and L. C. Wrobel, "Modelling, simulation and warming impact assessment of a domestic-size absorption solar cooling system," *Appl. Therm. Eng.*, vol. 22, no. 12, pp. 1313–1325, 2002, doi: 10.1016/S1359-4311(02)00054-6.

[6] N. Molero-Villar, J. M. Cejudo-López, F. Domínguez-Muñoz, and A. Carrillo-Andrés, "A comparison of solar absorption system configurations," *Sol. Energy*, vol. 86, no. 1, pp. 242–252, 2012, doi: 10.1016/j.solener.2011.09.027.

[7] M. S. A. Khan, A. W. Badar, T. Talha, M. W. Khan, and F. S. Butt, "Configuration based modeling and performance analysis of single effect solar absorption cooling system in TRNSYS," *Energy Convers. Manag.*, vol. 157, no. December 2017, pp. 351–363, 2018, doi: 10.1016/j.enconman.2017.12.024.

[8] Y. Hang, L. Du, M. Qu, and S. Peeta, "Multi-objective optimization of integrated solar absorption cooling and heating systems for medium-sized of fi ce buildings," *Renew. Energy*, vol. 52, pp. 67–78, 2013, doi: 10.1016/j.renene.2012.10.004.

[9] Y. Ma, S. C. Saha, W. Miller, and L. Guan, "Comparison of different solar-assisted air conditioning systems for Australian office buildings," *Energies*, vol. 10, no. 10, 2017, doi: 10.3390/en10101463.

[10] E. Asadi, M. G. da Silva, C. H. Antunes, and L. Dias, "A multi-objective

optimization model for building retrofit strategies using TRNSYS simulations, GenOpt and MATLAB," *Build. Environ.*, vol. 56, pp. 370–378, 2012, doi: 10.1016/j.buildenv.2012.04.005.

[11] A. Al-Alili, Y. Hwang, R. Radermacher, and I. Kubo, "Optimization of a solar powered absorption cycle under Abu Dhabi's weather conditions," *Sol. Energy*, vol. 84, no. 12, pp. 2034–2040, 2010, doi: 10.1016/j.solener.2010.09.013.

[12] J. A. Demko, *High-temperature superconducting cable cooling systems for power grid applications*. Elsevier Ltd, 2015.

[13] Y. a. Çengel, "Thermodynamics: An Engineering Approach," McGraw-Hill, 2004.

[14] R. Nikbakhti, X. Wang, A. K. Hussein, and A. Iranmanesh, "Absorption cooling systems – Review of various techniques for energy performance enhancement," *Alexandria Eng. J.*, vol. 59, no. 2, pp. 707–738, 2020, doi: 10.1016/j.aej.2020.01.036.

[15] A. Ghafoor and A. Munir, "Worldwide overview of solar thermal cooling technologies," *Renew. Sustain. Energy Rev.*, vol. 43, pp. 763–774, 2015, doi: 10.1016/j.rser.2014.11.073.

[16] V Mittal, KS Kasana, and NS Thakur, "The study of solar absorption air-conditioning systems," *J. Energy South. Africa @BULLET*, vol. 16, no. 4, pp. 59–66, 2005.

[17] J. A. Duffie and W. A. Beckman, *Wiley: Solar Engineering of Thermal Processes, 4th Edition - John A. Duffie, William A. Beckman*. 2013.

[18] M. Balghouthi, M. H. Chahbani, and A. Guizani, "Solar powered air conditioning as a solution to reduce environmental pollution in Tunisia," *Desalination*, vol. 185, no. 1–3, pp. 105–110, 2005, doi: 10.1016/j.desal.2005.03.073.

[19] M. Balghouthi, M. H. Chahbani, and A. Guizani, "Feasibility of solar absorption air conditioning in Tunisia," *Build. Environ.*, vol. 43, no. 9, pp. 1459–1470, 2008, doi: 10.1016/j.buildenv.2007.08.003.

[20] L. A. Chidambaram, A. S. Ramana, G. Kamaraj, and R. Velraj, "Review of solar cooling methods and thermal storage options," *Renew. Sustain. Energy Rev.*, vol. 15, no. 6, pp. 3220–3228, 2011, doi: 10.1016/j.rser.2011.04.018.

[21] O. Marc, J. P. Praene, A. Bastide, and F. Lucas, "Modeling and experimental

validation of the solar loop for absorption solar cooling system using double-glazed collectors," *Appl. Therm. Eng.*, vol. 31, no. 2–3, pp. 268–277, 2011, doi: 10.1016/j.applthermaleng.2010.09.006.

[22] D. S. Kim and C. A. Infante Ferreira, "Solar refrigeration options - a state-of-the-art review," *Int. J. Refrig.*, vol. 31, no. 1, pp. 3–15, 2008, doi: 10.1016/j.ijrefrig.2007.07.011.

[23] X. Garcı, "Solar absorption cooling in Spain : Perspectives and outcomes from the simulation of recent installations ´ a Casals *," vol. 31, pp. 1371–1389, 2006, doi: 10.1016/j.renene.2005.07.002.

[24] J. A. Duffie, W. A. Beckman, and J. McGowan, " Solar Engineering of Thermal Processes ," *Am. J. Phys.*, vol. 53, no. 4, pp. 382–382, 1985, doi: 10.1119/1.14178.

[25] S. A. Kalogirou, "Optimization of solar systems using artificial neural-networks and genetic algorithms," *Appl. Energy*, vol. 77, no. 4, pp. 383–405, 2004, doi: 10.1016/S0306-2619(03)00153-3.

Chapter 3: Research Methodology

3.1 Overview:

In the previous chapter a detailed literature review regarding solar cooling systems, solar collectors and thermal cooling systems was presented. This chapter is about the methodology adopted to carry out research on building integrated solar thermal cooling system for Pakistan's climate conditions.

Designing a new solar cooling facility is a complex task and one can face many problems. Such as proper sizing of the components, also, lack of standard specification and configurations due to variations in climate conditions and building characteristics makes designing a difficult job. Every case is different and specific, and detailed study and optimization is required to achieve maximum efficiency of the cooling system. Different software's and tools are used by researchers for solar cooling system studies worldwide [1].

This research study aimed to evaluate energy performance of a cold storage building integrated with solar assisted absorption cooling system. The goal is to use solar energy as hybrid energy source with conventional energy systems to meet the cooling demands of a cold storage with actual construction materials and standards used in Pakistan. The two main techniques available for the study of solar cooling system are either by experimental study or by dynamic simulation method. But as there is no experimental setup or installed system in cold storages in Pakistan; dynamic simulation will therefore be the adopted methodology for this study.

For the dynamic simulation of the cold storage building integrated with solar absorption cooling system, a realistic 3D cold storage building model with actual building characteristics (e.g. construction standards, materials, size etc.) will be chosen and the solar cooling system will be sized accordingly, so that it can maintain the storage temperature at the required set point all the time. For calculating the cold storage cooling load, the internal gains by workers, equipment's and banana load will be considered. Suitable components for the solar cooling system will be selected and will be optimized for the most efficient configuration and operational parameters. The optimization will consider the main system variables which have effect on the energy performance (e.g.

collector area, storage tank volume etc.) and the criteria for optimization will be on minimum installation and operational cost of solar loop based.

3.2 Approach of the study.

The steps followed for modelling, simulation and optimization of this study are summarized below:

- An existing cold storage building model is created in Google Sketchup and imported to TRNSYS. Building materials and geometry (walls and windows) are assigned in Trnsys3d.
- Weather data of the location is imported from the TRNSYS library as a TMY file. It consists of annual solar beam and diffused radiation, ambient temperature (both dry bulb and wet bulb), relative humidity and wind speed etc.
- Cold storage internal gains and operational conditions are defined in TRNSYS to calculate the maximum cooling load demand and estimate the size of the cooling system.
- Suitable components from the TRNSYS library are imported and connected with each other in the simulation studio. Main components selected are
    i. Hot water fired LiBr – H_2O absorption chiller
    ii. Evacuated tube solar thermal collectors
    iii. Stratified hot water storage tank
    iv. Boiler (Auxiliary heater)
    v. Cooling tower
    vi. Pumps, fan, and controllers
- Components and weather data are assembled and connected in two different configurations (e.g. C1 and C2).
- Comparison of the two configuration is done on installation and operational cost. And both configurations are optimized on minimum operational cost.

3.3 Building model description

The building selected for this study was a banana cold storage facility located at Mardan, Khyber Pakhtunkhwa Pakistan. The cold storage consists of 4 walls. The specifications

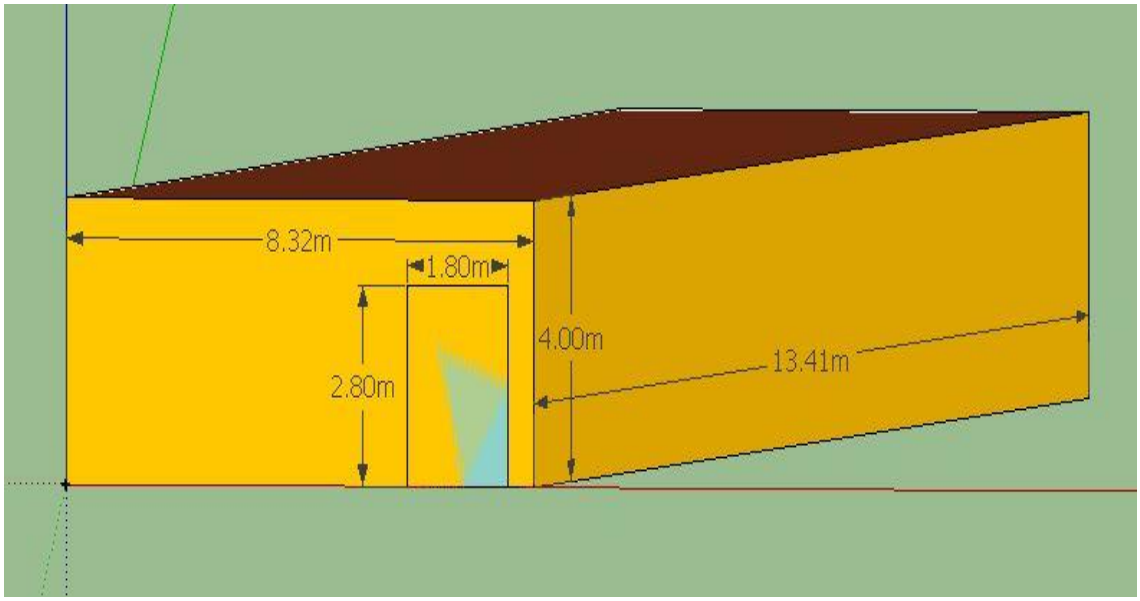

Figure 3.1: Trnsys 3-D model of storage building front view

and dimensions of which are given in the Table 3.1. The walls of the selected building are made of 0.2 m thick common bricks with 0.012 m plaster layer on the inside. Polystyrene insulation of thickness 0.051 m and steel cladding of thickness 0.005 m was also installed on the inside to minimize losses from the building envelop. The roof of the building is made of 0.1 m heavy weight concrete along with 0.1 m layer of common brick. To minimize thermal loses polystyrene and steel cladding were also installed with 0.051 m and 0.005 m thickness, respectively. Floor is made of 0.13 m thick layer of heavy weight concrete.

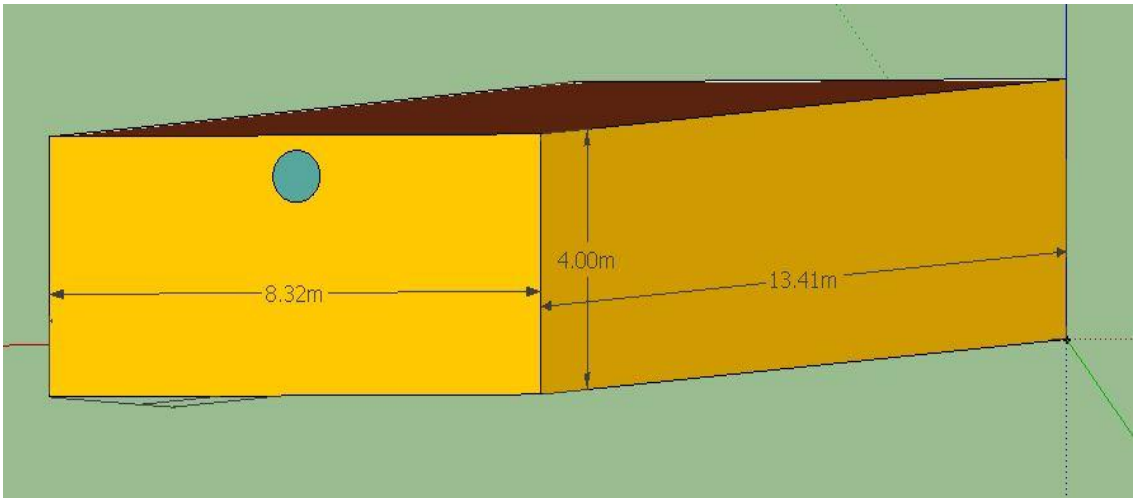

Figure 3.2: Trnsys 3-D model of Cold Storage building back view

TRNSYS supported Google Sketchup was used to model the existing cold storage building. The model used 3D building geometry for a space to be used in solar thermal cooling simulations. Trnsys3d plug-in is used to add geometric information into the building model. In the simulation studio, ‘’Type56’’ component was used for the building model. The selected cold storage building is a single zone model as shown in the Fig 3.1 and Fig 3.2, some other parameters are as follow:

Floor area = 78.89 m^2

Zone Volume (V) = 315.57 m^3

Location: 34.1989° N, 72.0231° E

Table 3-1: Dimensions of the Cold Storage building

Sr. No	Orientation	Length [L] (m)	Height [H] (m)	Gross Area (m^2)	Door Area (m^2)	Net Area (m^2)
1	N	8.32	4	33.28	-	33.28
2	SE	13.41	4	53.64	-	53.64
3	S	8.32	4	33.28	5.04	28.24
4	NW	13.41	4	53.64	-	53.64

3.3.1 Mathematical description of Type56

The heat gain by building thermal zone are described in this section. The building model in Type 56 is an energy balance model. Fig. 3.3 shows that the temperature of a zone depends upon different heat gains.

3.3.1.1 Convective heat flux to the air zone

The total heat gain Q_i of a zone is the summation of all kind of heat transfer to or from the thermal zone and can be calculated using Eq. 1.

$$\dot{Q}_i = \dot{Q}_{surf,i} + \dot{Q}_{inf,i} + \dot{Q}_{solar,i} + \dot{Q}_{g,c,i} + \dot{Q}_{vent,i} + \dot{Q}_{cplg,i} + \dot{Q}_{ISHCCI,i} \quad (1)$$

Where,

$\dot{Q}_{surf,i}$ is the convective heat gain from the surfaces

$\dot{Q}_{inf,i}$ is the infiltration gains due to the flow of air from the outside, given by

$\dot{\dot{Q}}_{inf,i} = \dot{V}\ \rho\ c_p\ (\ T_{out} - T_{air}\ )$

$\dot{Q}_{solar,i}$ is the fraction of solar radiation which enters the air zone through external windows.

$\dot{Q}_{g,c,i}$ are the internal convective heat gains (e.g. by people, equipment, radiators etc.)

$\dot{Q}_{vent,i}$ is the ventilation heat gain (e.g. air flow for a user defined source, like an HVAC system, given by

$\dot{Q}_{vent,i} = \dot{V}\ \rho\ c_p\ (\ T_{ventilation,i} - \ T_{air}\ )$

$\dot{Q}_{cplg,i}$ is the convective heat gains from due to the airflow from boundary condition, given by

$\dot{Q}_{cplg,i} = \dot{V}\ \rho\ c_p\ (\ T_{zone,i} - \ T_{air}\ )$

$\dot{Q}_{ISHCCI,i}$ is the absorbed solar radiation on all internal shading devices

3.3.1.2 Cooling Load Calculation

In most of the studies the cooling load of the building is already known. But for this specific case, the cooling load was calculated using TRNSYS. The cold storage cooling load was based on room envelop conduction and internal gains. In cold storages the primary cooling load is the heat generated by the products kept in the cold storage. The gains from the occupancy (per person of the labor force) were set according to ISO7730 standard with heavy work, lifting activities of 470W (165W sensible load and 300W latent load) and there were total 8 workers counted for the study. The artificial lightning heat

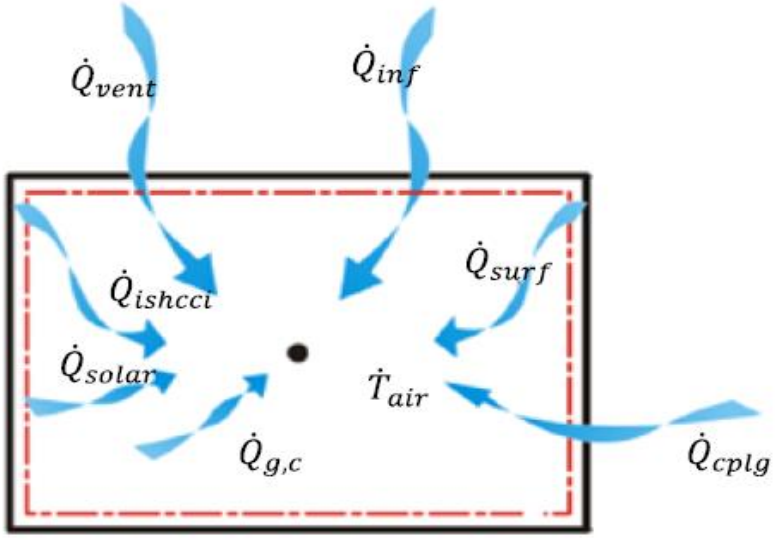

Figure 3.3: Heat Balance of the building thermal zone

gain was 10 W/m^2. The gains from the product (e.g. banana) was calculated according to the Eq. 2 [2]

$$\dot{Q}_i = \dot{m}\, C_v\, \Delta T \quad (2)$$

Where, $\dot{m}$ is the mass of the product kept for cooling period (Kg/Time), C_v is the specific heat of the product kept (e.g. 2.292 kJ/kg K for banana) [3] and ΔT is the temperature difference

3.4 System Description

Solar cooling system for cold storage was modelled with two different configurations and was compared and analyzed. Both configurations are discussed below.

3.4.1 Configuration -1

In Configuration-1 (C-1), base fluid (e.g. water) from the solar thermal collector enters stratified water storage tank. Water then passes through an auxiliary backup heater. A thermostat installed in parallel continuously examines the temperature of water leaving the hot water storage tank and if the water temperature while leaving the storage tank is less than desired level (e.g. 90^0 C), then the auxiliary heater turns on and raise the temperature to the required level. After auxiliary heater, water enters absorption chiller at a constant temperature of 90^0 C where it delivers heat to the chiller and returns to the storage tank and then to the solar collectors and the cycle continues. A controller monitors the in and out temperatures of collectors and controls the pump flow. If the temperature

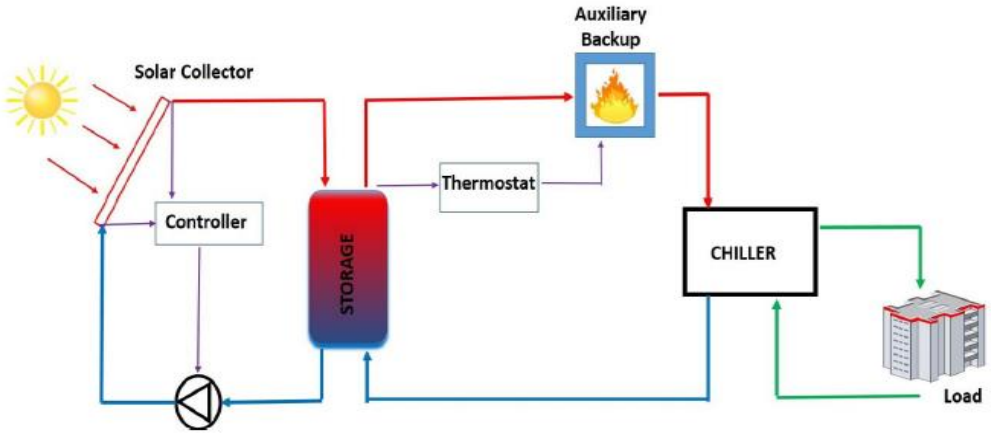

Figure 3.4: Configuration-1 (C1) for solar absorption cooling system

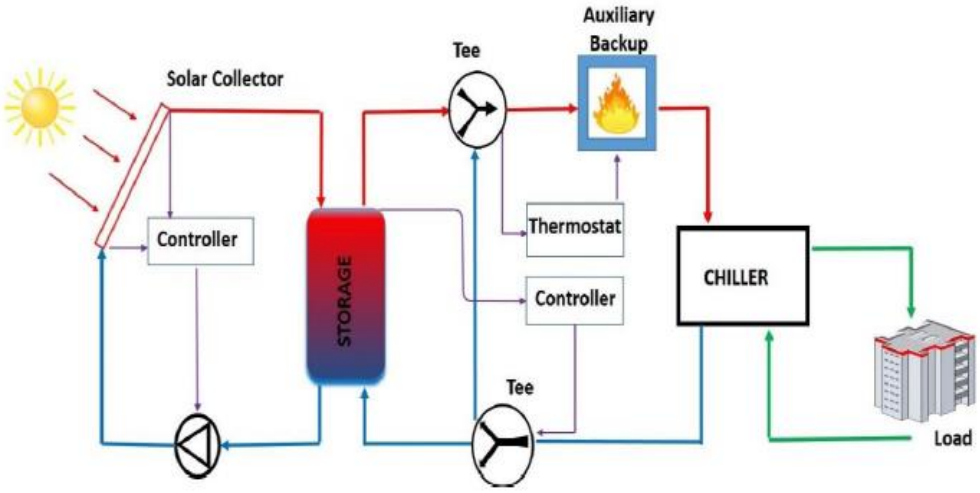

Figure 3.5: Configuration-2 (C2) for solar absorption cooling system

of the water come from out of collector is higher than the collector inlet temperature, the controller turns pump on, otherwise it remains off.

3.4.2 Configuration -2

In Configuration-2 (C-2), base fluid (e.g. water) from the solar thermal collector enters stratified water storage tank. If the temperature of the water leaving the stratified storage tank is below the required temperature (e.g. 90^0 C), water does not enter auxiliary boiler loop and it continues to circulate in the solar loop. Water leaving the absorption chiller is diverted to Tee mixer where it is either directed to the auxiliary boiler directly or to the storage tank. A tee junction and a controller is used for this purpose. The controller diverts water to the storage tank if the required temperature (e.g. 90^0 C) is available in the storage tank otherwise the flow is diverted to the auxiliary heater.

3.5 TRNSYS Model

Both configuration models (C-1 and C-2) are modelled by importing various components from the library and connecting them as shown in the Fig 3.6 and 3.7.

In modelling of the system following simplifying assumptions are taken.

- Effect of boiling or freezing of water are not considered in this study
- No pressure relief valve is installed and thereby loss of mass of water is not considered.
- Power consumed in components such as circulating pumps (other than solar loop pump) and controllers are not considered.

- The storage tank is kept in outdoor conditions to minimize thermal energy losses.

3.6 System Components Description

A simplified process flow diagrams of both configurations are shown in the Fig 3.6 and 3.7. It should also be noted that connecting lines in the diagram represent logical connections in the simulation rather than physical pipes connections etc.

3.6.1 Evacuated Tube Collector

An evacuated tube solar collector of Type 71 is used in this study for TRNSYS simulation. The solar collector's efficiency depends on the collector inlet, outlet, or average temperature. In Type 71 input parameters, efficiency mood, one (1) is selected if the collector efficiency parameters are presented as a function of the collector inlet temperature. Two (2) is selected if the collector efficiency parameters are presented as a function of collector average temperature. Three (3) is selected if the efficiency parameters are function of collector outlet temperature. The efficiency of a solar collector is given by Eq. 3.

$$\eta_{collector} = \alpha_0 - \alpha_1 \frac{(\Delta T)}{I_T} - \alpha_2 \frac{(\Delta T)^2}{I_T} \quad (3)$$

Where, α_0 is the optical efficiency, α_1 and α_2 are coefficients of heat loss

ΔT is the difference between fluid inlet temperature to the solar thermal collector and the ambient temperature ($T_{in} - T_{amb}$).

I_T is the incident total solar radiation

The values of the above-mentioned parameters are provided by the solar collector's manufacturers and are listed in the Table 3.2.

3.6.2 Absorption Chiller

A hot water fired single effect absorption chiller (Type 107) is used in this study. Hot water fired implies that the energy delivered to the chiller's generator comes from the hot water stream. The performance of an absorption chiller is determined in terms of Coefficient of performance (COP) of the chiller. The COP of the absorption chiller is given by:

Table 3-2: Parameters of evacuated tube collectors

Parameters	Description	Unit	Value
C_p	The specific heat capacity of working fluid	kJ/ (kg K)	4.190
η	Efficiency mood	-	1 ($T_{in} - T_{amb}$).
α_0	Intercept Efficiency	-	0.7
α_1	Efficiency Slope	(kJ/hr. m^2 K)	10
α_2	Efficiency Curvature	(kJ/hr. m^2 K^2)	0.03

$$COP = \frac{\dot{Q}_{chw}}{\dot{Q}_{hw}} \quad (4)$$

Where,

$\dot{Q}_{chw}$ is the energy removed from the chilled water stream.

$\dot{Q}_{hw}$ is the energy supplied by the hot water stream to the generator of chiller.

The total energy that must be removed by the chiller from the chilled water stream to bring it back from its entrance temperature to the set point temperature is calculated by Eq. 5

$$\dot{Q}_{chw} = \dot{m}_{chw} Cp_{chw} (T_{chw,in} - T_{chw,set}) \quad (5)$$

The amount of energy supplied to the chiller from the hot water stream can be calculated using Eq. 6.

$$\dot{Q}_{hw} = \frac{Capacity_{rated}}{COP_{rated}} f_{DesignEnergyInput} \quad (6)$$

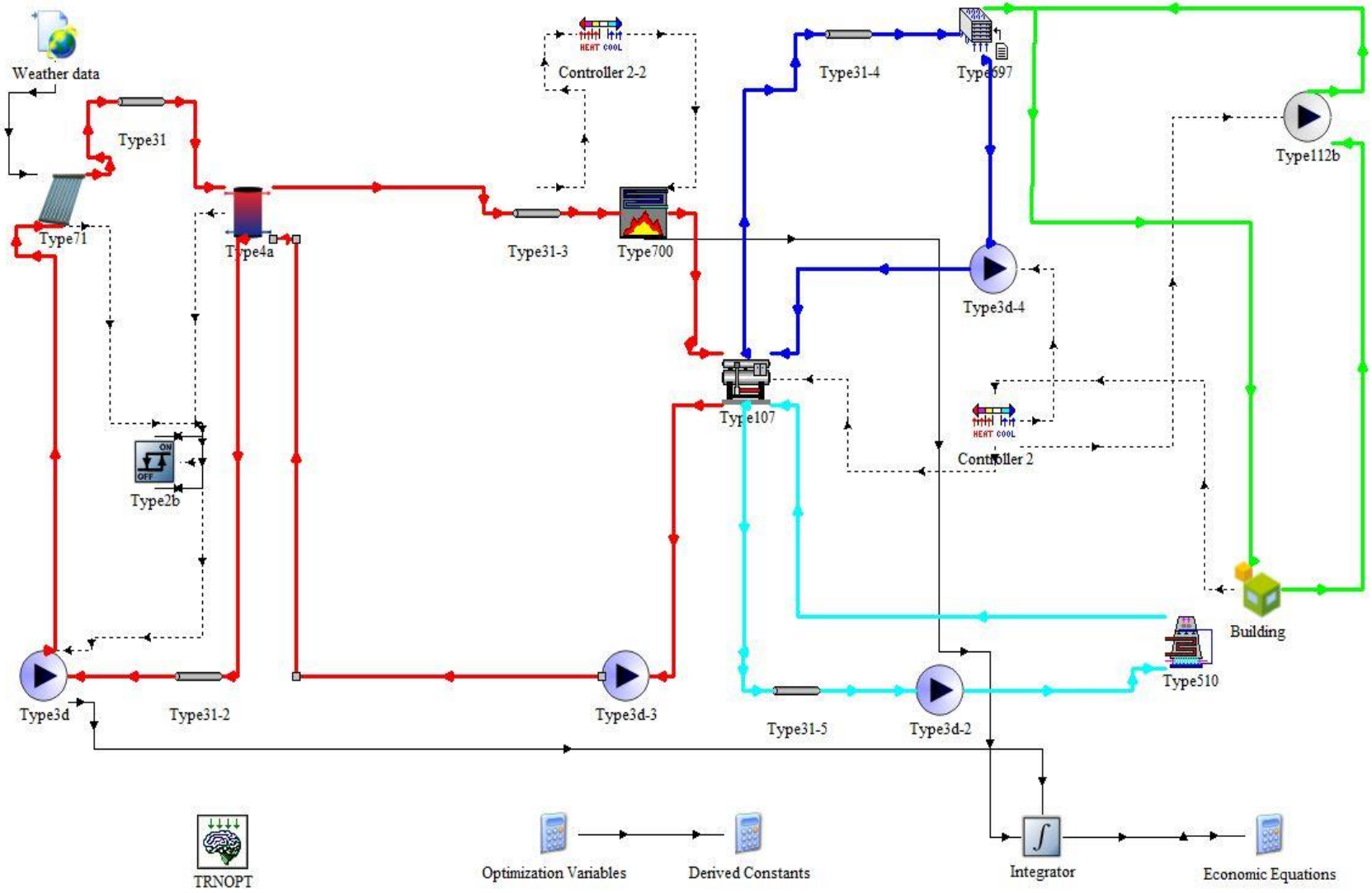

Figure 3.6: Pictorial view of the TRNSYS model for C-1

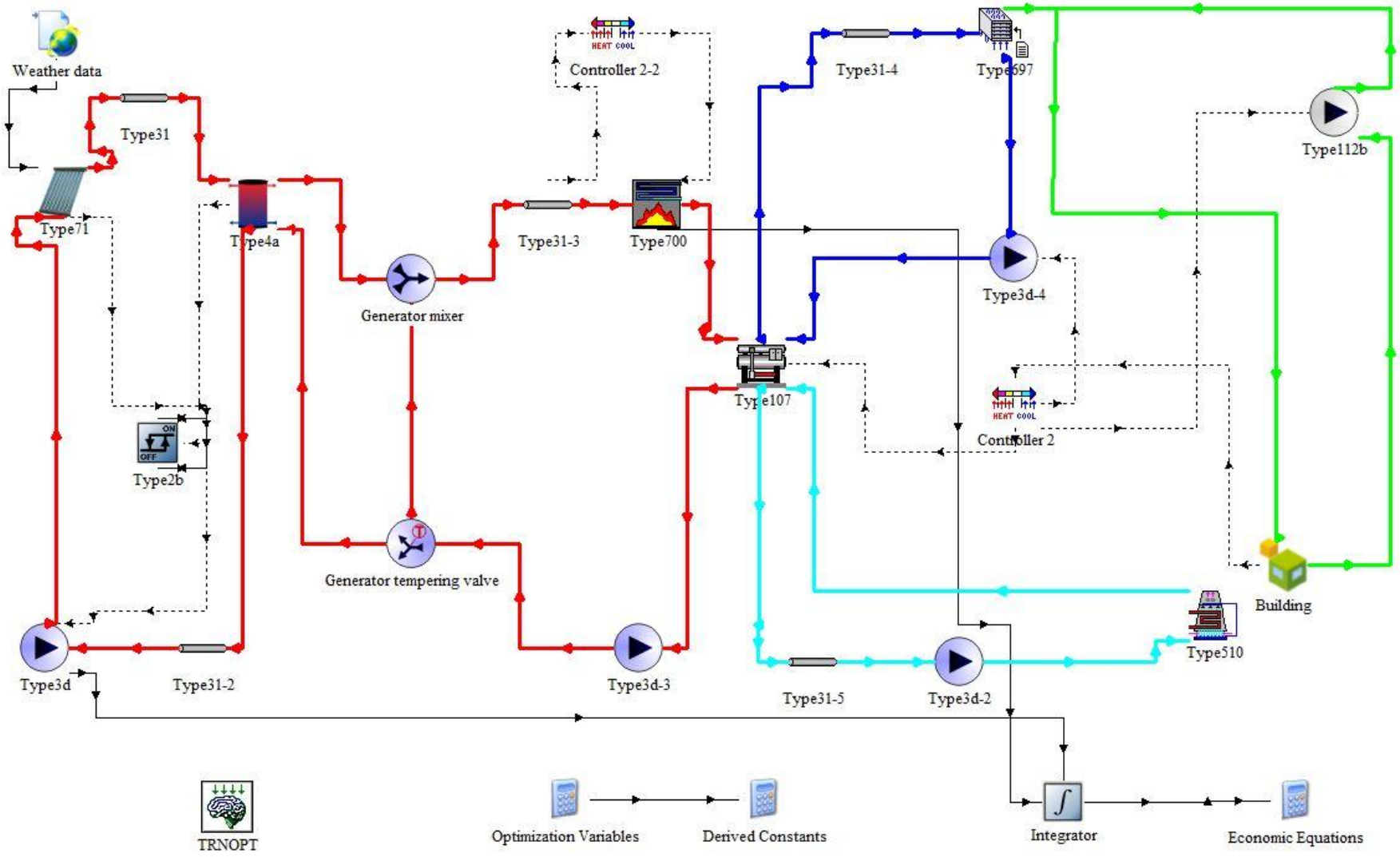

Figure 3:7: Pictorial view of TRNSYS model for C-2

Where,

$\dot{Q}_{hw}$ is the energy removed from the hot water stream.
$Capacity_{rated}$ is the rated cooling capacity of the chiller.
COP_{rated} is the rated COP of the machine.
$f_{DesignEnergyInput}$ is the fraction of input design energy required by the machine at present instant.
The energy rejection to the cooling tower required can be calculated by using Eq. 7

$$\dot{Q}_{cw} = \dot{Q}_{chw} + \dot{Q}_{hw} \quad (7)$$

Where $\dot{Q}_{cw}$ is the energy removed from the system by cooling tower.

A hot water fired LiBr-H_2O based chiller was used in this study. The technical data was obtained from a china-based company (e.g. Shandong Lucy New Energy Technology Co., Ltd)[4]. The technical parameters are listed in the Table 3.3

3.6.3 Hot Water Storage Tank

A stratified hot water storage tank (Type 4a) was used to simulate thermal storage tank in this study. It is a storage tank with fixed inlets and uniform losses with an auxiliary heating system. The fluid in the tank is hot at the top and is cold at the bottom. The tank is divided into ten equal nodes. And it is assumed that losses from each node of the tank are equal. The hot water from the thermal collector enters to the top of the tank and exit from the top to the chiller. The cold side water from the chiller enters the tank at the bottom and exits the tank bottom towards the collector.

For heat loss calculations from the storage tank it is assumed that the tank is well insulated, and the ambient temperature is considered as an input for the heat loss calculation from the storage tank. The tank average heat loss-coefficient is taken to be 0.167 kJ. Hr^{-1} $m^{-2}K^{-1}$.

3.6.4 Auxiliary Heater

An auxiliary boiler (Type 700) is installed after hot water storage tank in the simulation model. It is installed in the loop that if the required temperature is not achieved by the solar collectors then the controller will turn on the boiler and will heat the fluid to the required generator temperature. It also calculates the required input energy to elevate the input fluid temperature to the set point temperature using Eq. 8.

Table 3-3: Technical parameters of hot water fired absorption chiller

Model		Unit	RXZ-23
Capacity		kW	23
Hot Water	Flow rate	m^3/h	5.8
	Inlet/Outlet Temp.	^{0}C	90 / 85
	Inlet/Outlet Dia.	mm	DN40
Chilled Water	Flow rate	m^3/h	4
	Inlet/Outlet Temp.	^{0}C	15/10 (12/7)
	Inlet/Outlet Dia.	mm	DN32
Cooling Water	Flow rate	m^3/h	10
	Inlet/Outlet Temp.	^{0}C	30
	Inlet/Outlet Dia.	mm	DN40
Dimensions	Length	mm	1010
	Width	mm	785
	Height	mm	1622
Power Consumption		kW	0.3
Shipping weight		kg	730

$$\dot{Q}_{need} = \dot{m}_{fluid} Cp_{fluid} (T_{set} - T_{in}) \quad (8)$$

The device will not calculate energy if the $\dot{Q}_{need}$ is negative for instance a case where inlet temperature is higher than the set point temperature. The required energy by the fluid is controlled by the total capacity of the auxiliary boiler

Once, the required energy by the fluid is determined, the amount of fuel required can also be calculated by Eq. 9.

$$\dot{Q}_{fuel} = \frac{\dot{Q}_{need}}{\eta_{boiler}} \quad (9)$$

3.7 System Performance factors

i. Lowest Life Cycle Cost

The size of solar thermal collector and hot water storage tank are manipulated to find the lowest life cycle cost of the system. Larger collector area and storage tank volume will

reduce the auxiliary backup heater consumption thus reducing the operational cost of the system, but in the mean while it also increases the installation cost of the system. Multiple variables optimization is carried out using GenOpt optimization tool of TRNSYS and the following steps are being followed.

- **Choosing the input TRNSYS file to be optimized**.
- **Choosing the variables to be optimized**.

  In this study collector area and storage tank volume are the two variables selected for optimization
- **Specifying variables information**

  The variables are specified as ‘’continuous’’ or ‘’discreet’’ and then a range is identified for each variable.
- **Selection of the error function**

  A simulation output is selected which will be minimized during optimization process. In this study the following cost equation was selected as a simulation output.

  COST_SOLAR = AREA_COLL*COST_M2 + VOL_TANK * COST_M3 + LIFETIME*(Q_PUMP+Q_Aux)/3600*COST_KWH (10)

  Where,

  - COST_SOLAR is the total cost function of the study which will be minimized
  - AREA_COLL is the first variable which will be optimized in the defined range.
  - COST_M2 is the cost of the solar collector per square meter (e.g. 30,000 PKR).
  - VOL_TANK is the second variable which will be optimized in the defined range.
  - COST_M3 is the cost of storage tank per cubic meter (e.g. 80,000 PKR)
  - LIFETIME is the period for which the life cycle cost analysis is carried out.
  - Q_PUMP+Q_Aux is the summation of power consumption of the solar loop pump and the auxiliary backup boiler
  - COST_KWH is the cost of energy per kWh (e.g. 5.38 PKR) [6].
- **Choosing the optimization setting**

  First one is the maximum number of iterations for single simulation (e.g. 500 in this study). The second is the number of times the function value returns to the same value before the simulation terminates (e.g. 5 for this study)

- **Selection of optimization method**

  There are multiple options available for optimization method, but the selection is limited by the number and type of variables selected. Hooke-Jeeves algorithm is used in this study for optimization which is recommended method for continuous data [7].

3.8 References

[1] K. F. Fong, T. T. Chow, C. K. Lee, Z. Lin, and L. S. Chan, "Comparative study of different solar cooling systems for buildings in subtropical city," *Sol. Energy*, vol. 84, no. 2, pp. 227–244, 2010, doi: 10.1016/j.solener.2009.11.002.

[2] S. K. Sari and N. W. Pratami, "Cooling load calculation of cold storage container for vegetables case study C Campus-UISI, Ngipik," *2018 Int. Conf. Inf. Commun. Technol. ICOIACT 2018*, vol. 2018-Janua, pp. 820–826, 2018, doi: 10.1109/ICOIACT.2018.8350726.

[3] H. T. HAMMEL, "Thermal properties of fur," *Am. J. Physiol.*, vol. 182, no. 2, pp. 369–376, 1955, doi: 10.1152/ajplegacy.1955.182.2.369.

[4] "CATALOG OF LUCY 2019.pdf." .

[5] R. Salgado, "Optimized solar cooling facility configurations for the mediterranean warm climate," p. 166, 2008.

[6] G. Regulatory *et al.*, "Oil and gas regulatoryauthority *****," no. I, 2019.

[7] M. Wetter, "Generic Optimization Program User Manual," *Energy*, no. c, pp. 1998–2011, 2011.

Chapter 4: Results and Discussion

4.1 Overview:

In the previous chapter 3, key components of a solar assisted absorption cooling system and their parameters were discussed to estimate the overall performance of two different configurations (e.g. C1 and C2). All the components were connected in TRNSYS simulation studio to obtain different combinations and were operated for realistic parameters referenced from literature. The solar cooling system was operated to maintain the condition space temperature of 15 ^{0}C inside a cold storage room of banana facility for the whole year. The system parameters for both configurations were optimized based on life cycle cost (e.g. installation and operational cost of energy input loop) using GenOpt optimization tool in TRNSYS. The optimum results were achieved by running optimization tool several hundred times and at the end the combination of parameters having minimum life cycle cost were selected as optimum parameters. After optimization, the results obtained are discussed here in detail.

4.2 Weather Data of Peshawar:

Figure 4.1 shows average monthly ambient temperature and percentage relative humidity for Peshawar region. It is evident from the figure that average monthly temperature is

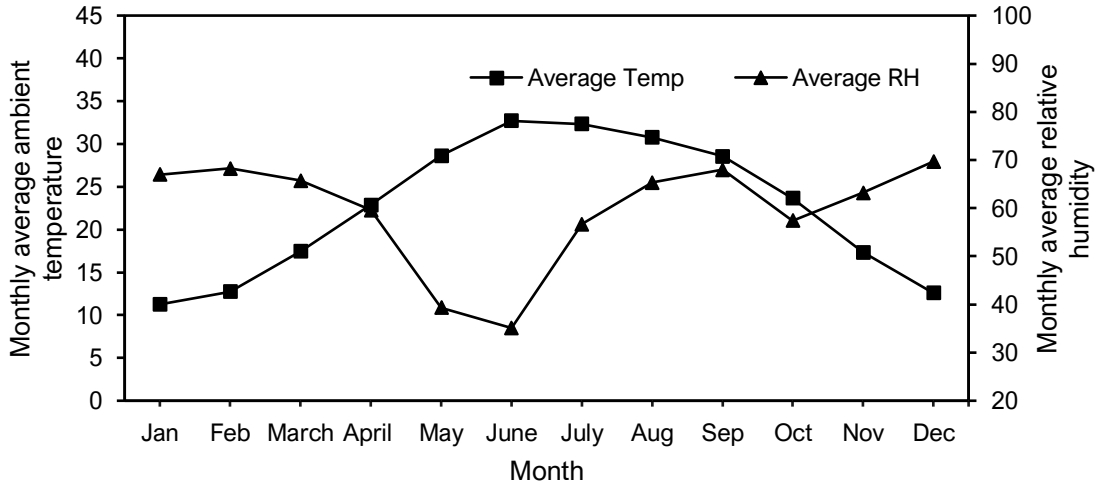

Figure 4.1: Monthly average ambient temperature and percentage relative humidity

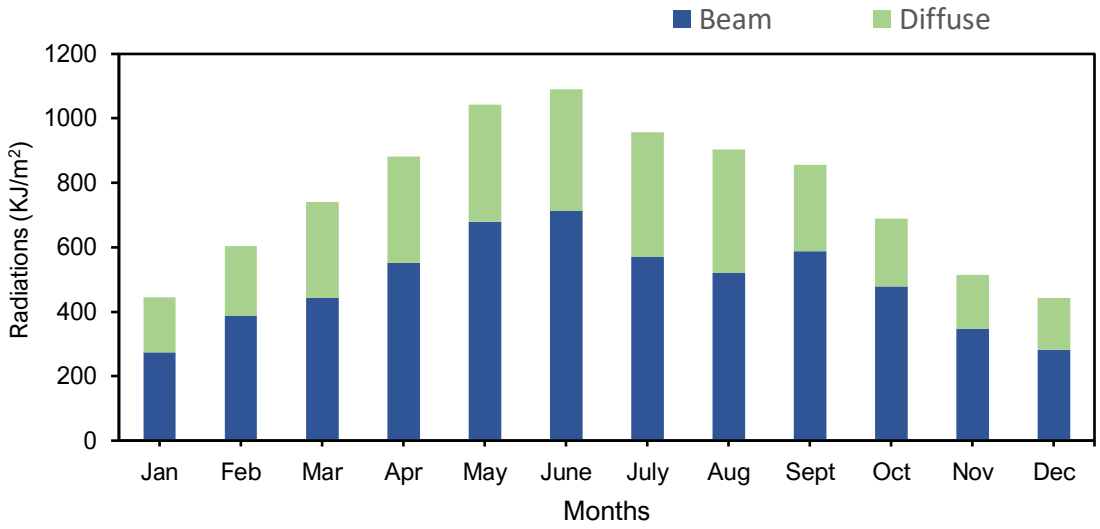

Figure 4.2: Average monthly Beam and Diffuse radiations

maximum in the month of June whereas, the percentage relative humidity is minimum for this month.

Figure 4.2 shows monthly radiation data for Peshawar including both beam and diffuse radiations. It is evident that total solar radiations are maximum in May and June having values of 1043 kJ/hr. m^2 and 1089 kJ/hr. m^2 respectively. Direct solar radiation is 678.36 kJ/hr. m^2 and 713.26 kJ/hr. m^2 while diffuse solar radiations are 364.75 kJ/hr. m^2 and 376.39 kJ/hr. m^2, respectively. These figures (e.g. Fig 4.1 and Fig 4.2) reveals the potential of renewable solar energy available when cooling requirements are maximum. Therefore, by using a SAC system these solar radiations can be utilized to achieve space cooling.

4.3 Cooling Load:

Finding the maximum cooling load demand of a building is essential for estimation of the size of a SAC system [1]. The cooling load of the selected building is calculated by running the simulations at a set point temperature of 15 ^{0}C. Figure 4.3 shows the hourly cooling load of cold storage building for whole year. It is evident from the figure that the maximum cooling load (e.g. 82400 kJ/hr.) is in the month of June.

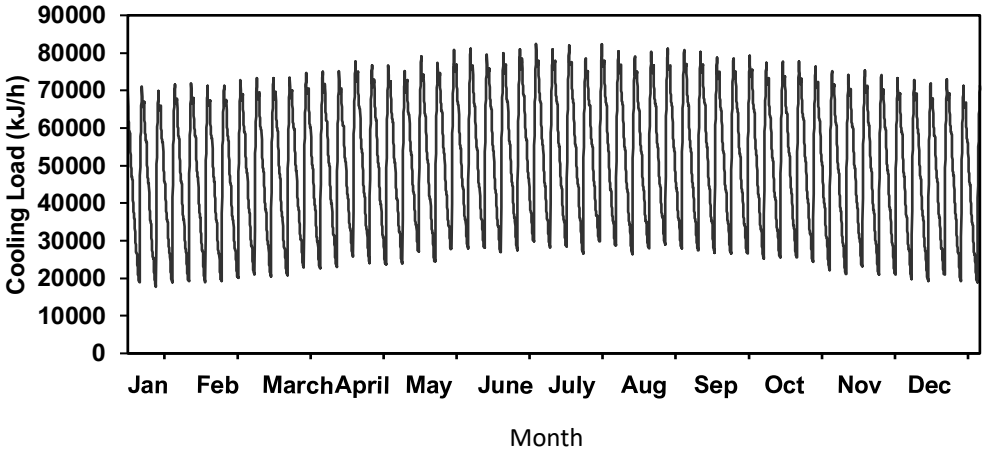

Figure 4.3: Hourly Cooling Load of the Cold Storage

Figure 4.4 shows the average monthly cooling load of the cold storage for whole year. It is evident from the figure that average cooling load is maximum in the month of May having a value of 63200 kJ/hr. while the lowest average cooling load demand is for the month of Sept having a value of 33500 kJ/hr. The cooling load demand for the rest of the months is approximately the same and remains in the range of 40000 kJ/hr. and 60000kJ/hr.

4.4 Optimization:

This study illustrates the optimization process of a solar absorption cooling system with evacuated tube collectors and hot water storage tank. In this study the area of collector array and the volume of the storage tank was manipulated to find the lowest cycle cost of

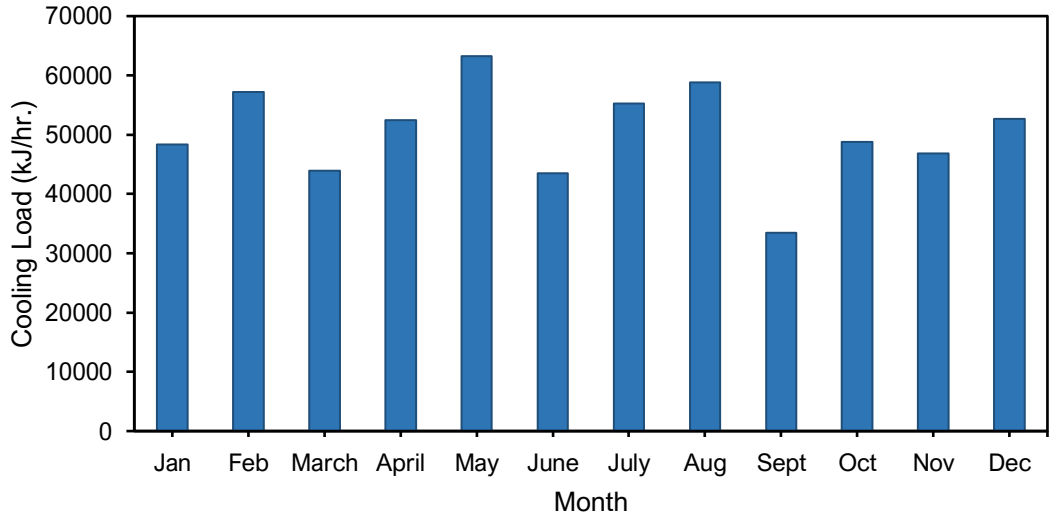

Figure 4.4: Average Monthly Cooling Load of the Cold Storage

the system. Studies shows that the larger collector area and storage tank volume can reduce the consumption of auxiliary boiler (and therefore the operational cost), but the savings are contrasted by the higher capital costs of the collector and the storage tank. To minimize the life cycle cost of the system the collector area and the storage tank volume was manipulated between 50 m^2 to 150 m^2 and 0.5 m^3 and 4 m^3 respectively for both configurations. To avoid getting "local minima'' and to get a "global minima" in the selected range of parameters, different initial points with increments of 10 m^2 and 0.5 m^3 were tested by running simulations multiple times. Table 4.1 shows the optimum values of parameters with minimum life cycle cost of both configurations for multiple combinations of initial parameters. Figure 4.5 shows the 5 smallest possible life cycle cost values of C1 for different combinations of storage tank volume and solar collector area. It can be evident from the figure that out of five smallest life cycle cost, four have an optimum collector area of 150 m^2 while the optimum storage tank volume is 1.99 m^3 for the lowest value of life cycle cost.

Table 4-1: Optimization results of Both Configurations

	Collector area			Volume of Tank			Configuration-1			Configuration-2		
Sr No.	Min (m^2)	Initial (m^2)	Max (m^2)	Min (m^3)	Initial (m^3)	Max (m^3)	Life Cycle Cost (PKR)	Area (m^2)	Volume (m^3)	Life Cycle Cost (PKR)	Area (m^2)	Volume (m^3)
1	50	50	150	0.5	0.5	4	28485997	149.6	0.99	28230209	54.1	0.50
2				0.5	1	4	28467407	150.0	0.53	10717950	58.9	2.29
3				0.5	1.5	4	28467407	150.0	0.53	14464551	50.4	1.55
4				0.5	2	4	28466277	150.0	1.99	12328053	50.0	2.18
5				0.5	2.5	4	28485869	150.0	2.58	13567088	50.6	2.52
6				0.5	3	4	28485997	149.6	0.99	10769527	56.0	3.30
7				0.5	3.5	4	28467407	150.0	0.53	13163989	50.1	3.50
8				0.5	4	4	28479164	149.8	0.83	13215817	50.0	4.00
9	50	60	150	0.5	0.5	4	28467407	150.0	0.53	11095737	84.0	2.20
10				0.5	1	4	28485997	149.6	0.99	28012567	60.1	0.99
11				0.5	1.5	4	28467407	150.0	0.53	13637322	60.1	1.50
12				0.5	2	4	28466277	150.0	1.99	10717950	58.9	2.29
13				0.5	2.5	4	28484579	150.0	2.34	12281006	59.6	2.50
14				0.5	3	4	28479164	149.8	0.83	10771174	59.9	2.85
15				0.5	3.5	4	28485997	149.6	0.99	10852920	60.0	3.50
16				0.5	4	4	28479164	149.8	0.83	10939954	62.8	4.00
17	50	70	150	0.5	0.5	4	28467407	150.0	0.53	12005619	84.9	1.99
18				0.5	1	4	28467407	150.0	0.53	14663182	66.5	1.30

19				0.5	1.5	4	28467407	150.0	0.53	13732309	71.4	1.49
20				0.5	2	4	28494125	150.0	1.29	11850242	70.0	2.03
21				0.5	2.5	4	28466277	150.0	1.99	10856387	69.6	5.25
22				0.5	3	4	28466277	150.0	1.99	10926930	70.6	3.00
23				0.5	3.5	4	28494125	150.0	1.29	11014735	69.4	3.80
24				0.5	4	4	28494125	150.0	1.29	11047543	70.4	4.00
25	50	80	150	0.5	0.5	4	28467407	150.0	0.53	12115376	92.0	1.90
26				0.5	1	4	28467407	150.0	0.53	12080622	86.9	2.01
27				0.5	1.5	4	28467407	150.0	0.53	13801555	79.5	1.50
28				0.5	2	4	28466277	150.0	1.99	11891989	80.4	1.95
29				0.5	2.5	4	28485869	150.0	2.58	10933238	74.8	2.23
30				0.5	3	4	28485997	149.6	0.99	11102177	81.9	3.33
31				0.5	3.5	4	28479164	149.8	0.83	11102512	77.0	3.55
32				0.5	4	4	28467407	150.0	0.53	11181161	79.9	4.00
33	50	90	150	0.5	0.5	4	28467407	150.0	0.53	7035703	116.1	2.75
34				0.5	1	4	28467407	150.0	0.53	12148948	93.8	1.91
35				0.5	1.5	4	28466277	150.0	1.99	14816088	91.5	1.45
36				0.5	2	4	28485997	149.6	0.99	12003453	90.3	2.00
37				0.5	2.5	4	28485869	150.0	2.58	11197672	89.9	2.85
38				0.5	3	4	28485997	149.6	0.99	11149195	88.0	3.10
39				0.5	3.5	4	28467407	150.0	0.53	11298913	90.5	3.50
40				0.5	4	4	28485997	149.6	0.99	11224648	88.0	3.70
41	50	100	150	0.5	0.5	4	28467407	150.0	0.53	12148948	93.8	1.91
42				0.5	1	4	28467407	150.0	0.53	6913482	112.7	2.85
43				0.5	1.5	4	28467407	150.0	0.53	14956582	101.1	1.40
44				0.5	2	4	28485997	149.6	0.99	12323189	102.1	2.00
45				0.5	2.5	4	28485997	149.6	0.99	11291193	98.4	2.38
46				0.5	3	4	28494125	150.0	1.29	11399735	100.6	3.05
47				0.5	3.5	4	28479164	149.8	0.83	11342157	98.4	3.65
48				0.5	4	4	28485997	149.6	0.99	6806052	102.9	3.93
49	50	110	150	0.5	0.5	4	28467407	150.0	0.53	6910290	111.6	2.85
50				0.5	1	4	28467407	150.0	0.53	15530938	106.1	1.30
51				0.5	1.5	4	28493282	150.0	3.20	8106342	108.6	2.40
52				0.5	2	4	28466277	150.0	1.99	9455814	108.4	2.09
53				0.5	2.5	4	28485869	150.0	2.58	8545499	109.8	2.49
54				0.5	3	4	28467407	150.0	0.53	8690323	114.8	3.20
55				0.5	3.5	4	28472800	150.0	2.88	6909076	109.9	3.46
56				0.5	4	4	28467407	150.0	0.53	7014019	111.9	3.90
57	50	120	150	0.5	0.5	4	28494125	150.0	1.29	9040277	129.1	2.01
58				0.5	1	4	28479164	149.8	0.83	8024509	123.0	1.90
59				0.5	1.5	4	28874477	129.2	0.53	8158726	124.8	2.03
60				0.5	2	4	28466277	150.0	1.99	9665842	118.4	1.90
61				0.5	2.5	4	28472800	150.0	2.88	8585799	120.7	2.58

62				0.5	3	4	28493282	150.0	3.20	7121889	119.9	2.95
63				0.5	3.5	4	28493282	150.0	3.20	7205383	121.3	3.59
64				0.5	4	4	28467407	150.0	0.53	6460354	120.3	3.95
65	50	130	150	0.5	0.5	4	28874477	129.2	0.83	9040277	129.1	2.01
66				0.5	1	4	28479164	149.8	0.83	8670739	114.9	2.40
67				0.5	1.5	4	28479164	149.8	0.83	8663305	126.5	1.70
68				0.5	2	4	28466277	150.0	1.99	9040277	129.1	2.01
69				0.5	2.5	4	28485869	150.0	2.58	9211874	129.0	2.49
70				0.5	3	4	28494125	150.0	1.29	7351537	126.9	3.30
71				0.5	3.5	4	28472800	150.0	2.88	7417762	128.8	3.53
72				0.5	4	4	28466277	150.0	1.99	6721610	131.3	4.00
73	50	140	150	0.5	0.5	4	28479164	149.8	0.83	8583162	140.8	1.90
74				0.5	1	4	28467407	150.0	0.53	9097828	148.0	2.15
75				0.5	1.5	4	28494125	150.0	1.29	8583162	140.8	1.90
76				0.5	2	4	28466277	150.0	1.99	9368855	141.0	2.09
77				0.5	2.5	4	28472800	150.0	2.88	10440344	139.9	2.40
78				0.5	3	4	28472800	150.0	2.88	6899038	140.5	3.03
79				0.5	3.5	4	28505465	150.0	3.78	6966565	140.7	3.81
80				0.5	4	4	28472800	150.0	2.88	6943027	140.1	4.00
81	50	150	150	0.5	0.5	4	28467407	150.0	0.53	9368855	141.0	2.09
82				0.5	1	4	28485997	149.6	0.99	8583162	140.8	1.90
83				0.5	1.5	4	28467407	150.0	0.53	9700499	148.8	1.71
84				0.5	2	4	28466277	150.0	1.99	9302688	147.0	2.80
85				0.5	2.5	4	28485869	150.0	2.58	8742691	149.3	2.57
86				0.5	3	4	28472800	150.0	2.88	7890092	147.9	3.38
87				0.5	3.5	4	28472800	150.0	2.88	7858560	148.4	3.45
88				0.5	4	4	28505465	150.0	3.78	6580760	127.2	4.00

Figure 4.6 shows the five lowest life cycle costs of C2 model. It is evident from the figure that the lowest life cycle cost occurs at 120.3 m^2 collector area and 3.95 m^3 storage tank volume. The lower collector area as compared to C1 model reduces initial installation cost thereby reducing the overall life cycle cost of the system.

4.4.1 Configuration-1 (C1)

The optimization process is performed eighty-eight times for each configuration with multiple combination of initial values. Throughout those results the global minima was obtained from taking 50 m^2 and 2 m^3 as initial values for collector area and storage tank volume. Figure 4.7 shows a GenOpt plot window with the results showing the life cycle cost.

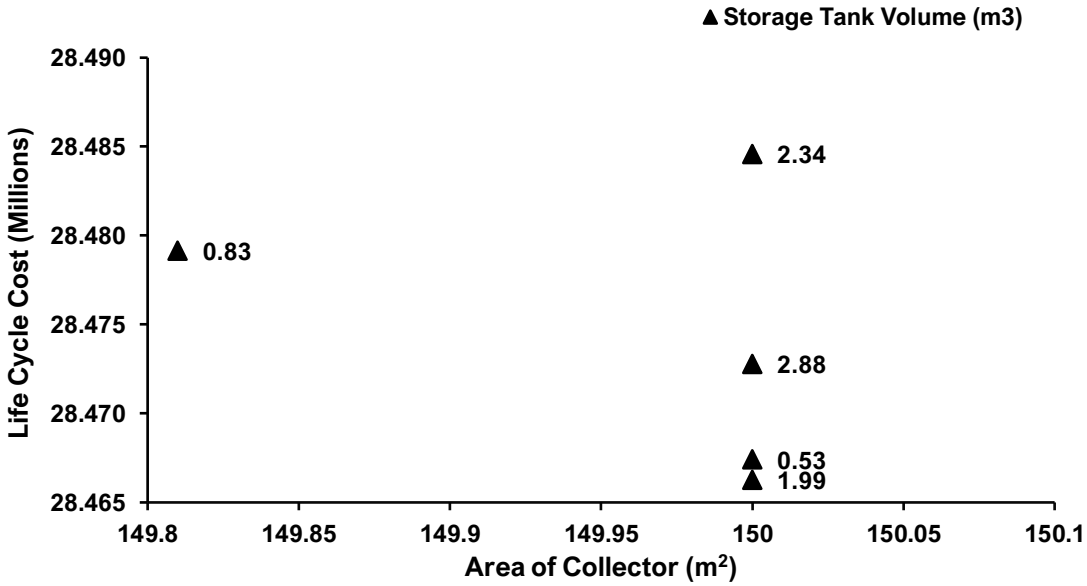

Figure 4.5: Lowest life cycle costs of C1

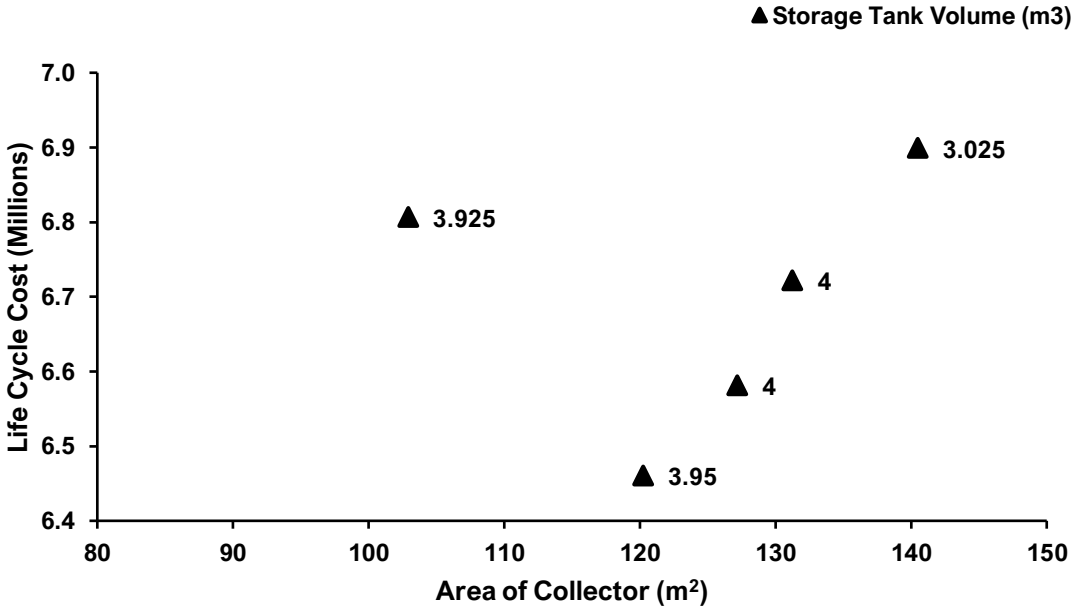

Figure 4.6: Lowest life cycle costs of C2

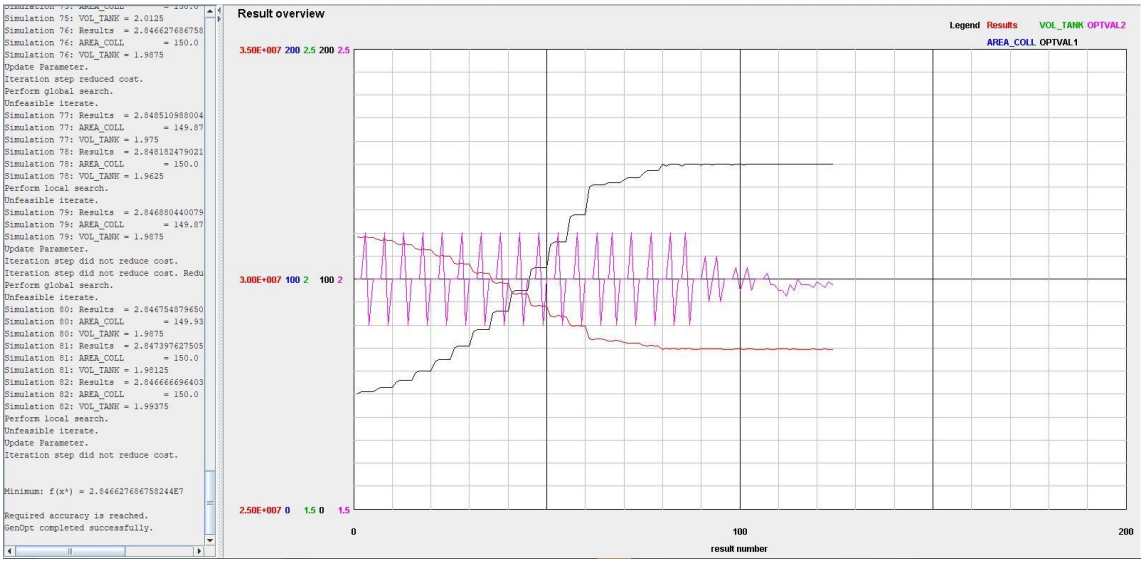

Figure 4.7: GenOpt's plot window for C-1

Figure 4.8 shows a detail graph of cost-based optimization of C1. Area of collector and storage tank volume are plotted on x and y axis respectively and life cycle cost on z axis. The increasing diameter of the sphere shows the progressive iteration steps. It can be seen from the graph that the lowest cost of 28466277 PKR occurs at 150 m^2 collector area and 1.98 m^3 storage tank volume.

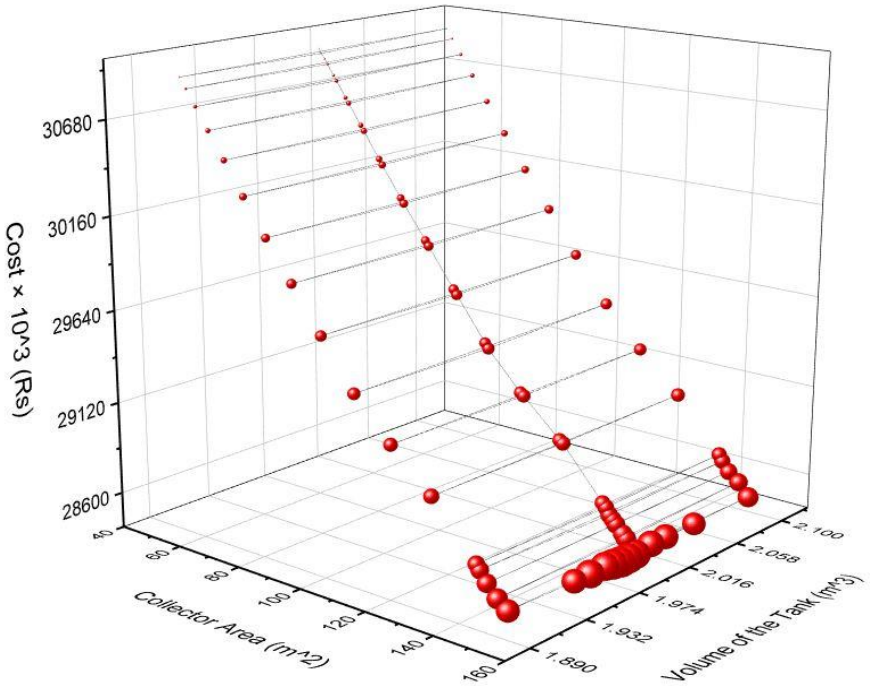

Figure 4.8: Cost Based Optimization Plot of C-1

4.4.2 Configuration-2 (C2)

Figure 4.9 shows GenOpt plot window showing the manipulation of area of collector and storage tank volume in the specified interval. the simulation starts from the initial value of 120 m^2 collector area and 4 m^3 storage tank volume. The simulation tends to reduce life cycle cost and terminates once the criteria is fulfilled.

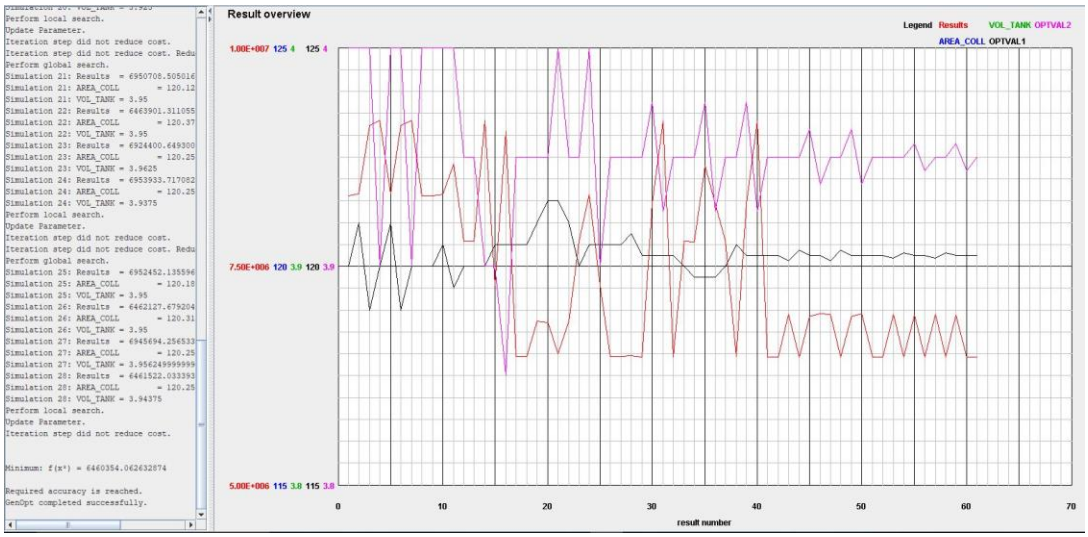

Figure 4.9: GenOpt's plot window for C-2

Figure 4.10 shows that a minimum life cycle cost of C2 is found to be 6460354 PKR having optimum collector area of 120.3 m^2 and storage tank volume to be 3.95 m^3. The reason for the life cycle cost so smaller than C1 is that most of the time in a year the hot water exit temperature from the absorption chiller is higher than the minimum operating temperature required by the absorption chiller. Hence, the flow divertor installed after absorption chiller diverts the flow towards the chiller instead of sending it to the storage tank. In the case when the flow is diverted back to the chiller the system avoids the mixing the hotter fluid returning from the chiller and the colder fluid present in the storage tank. Hence reducing the mixing losses and therefore, reducing the operational cost of the system.

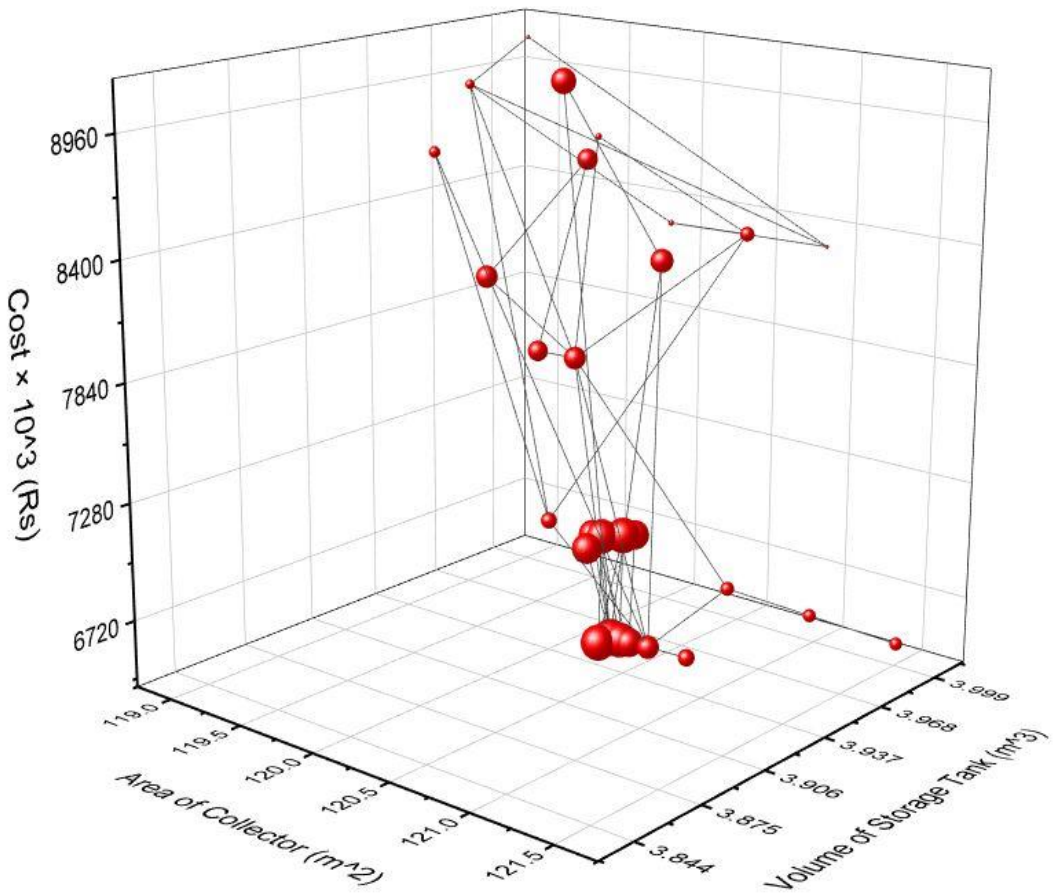

Figure 4.10: Cost based Optimization plot of C-2

4.5 Optimum Model:

After the collector's area and storage tank volume are optimized for minimum life cycle cost of both configurations the next step is to analyze different parameters of the optimum models for both configurations.

4.5.1 Fluids Temperature and Heat Transfer Rates

The fluid inlet and outlet temperatures at various points and the heat transfer rates at different components were analyzed for both configurations for a typical week of June having the highest cooling load demand throughout the year. Figure 11 and 12 shows the inlet and outlet temperature of the absorption chiller (e.g. $T_{g,i}$ and $T_{g,o}$), the collector outlet temperature ($T_{col,o}$), the storage tank outlet temperature ($T_{st,o}$), the chilled water inlet and outlet temperature ($T_{ch,i}$ and $T_{ch,o}$), the cooling water inlet and outlet temperature T_{cw} (,$_i$ and $T_{cw,o}$) and the conditioned space temperature. It is evident from the figure 4.11 and 4.12

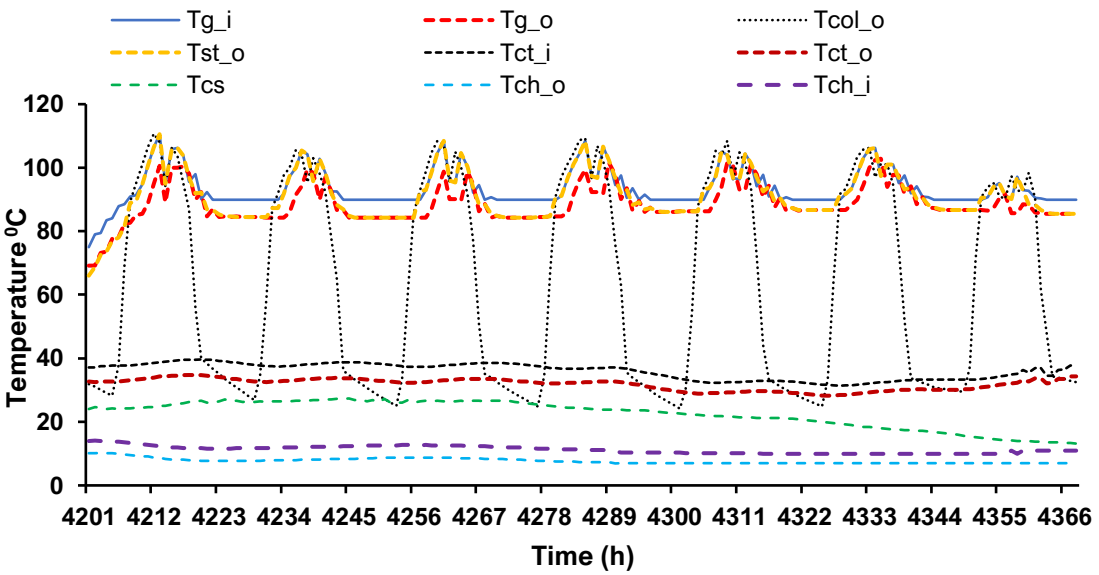

Figure 4.6: Variation of fluids temperature in a typical week of June for C1

that the difference in the collector output temperature and storage tank output temperature is significant in C1 as compared to C2. The storage tank output temperature remains below the chiller required temperature of 90 ^{0}C for most of the simulation time in the week. While in C2 on the other hand, the storage tank outlet temperature remains higher than the chiller required temperature for the last couple of days of the week.

From the same simulation time, the resulting pattern of COP, fraction of the chiller nominal capacity and the heat energy rates of the solar thermal collector (Q_{solar}), auxiliary boiler

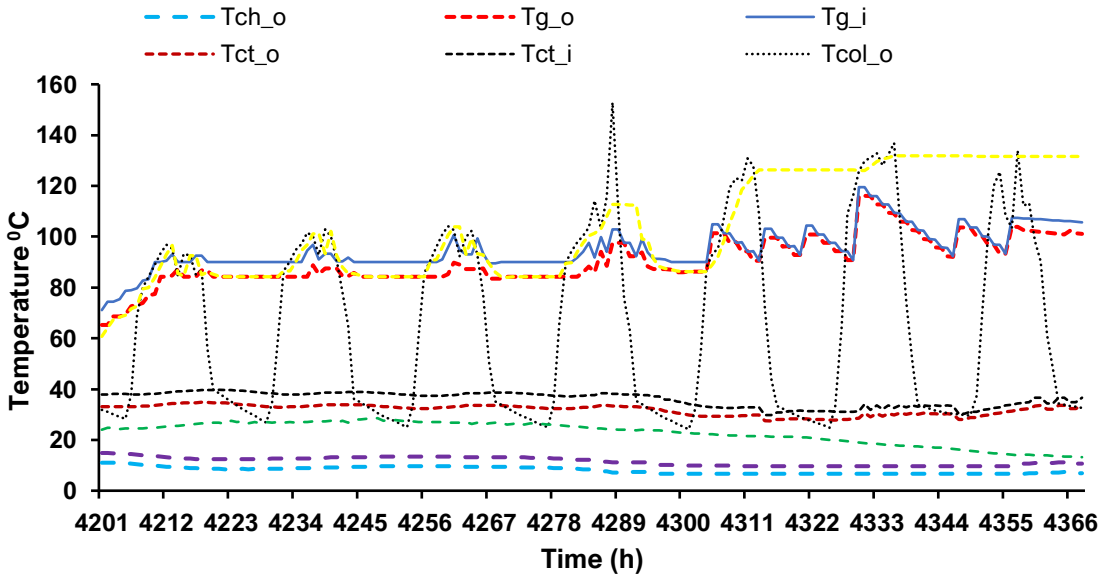

Figure 4.7: Variation of fluid temperature in a typical week of June for C2

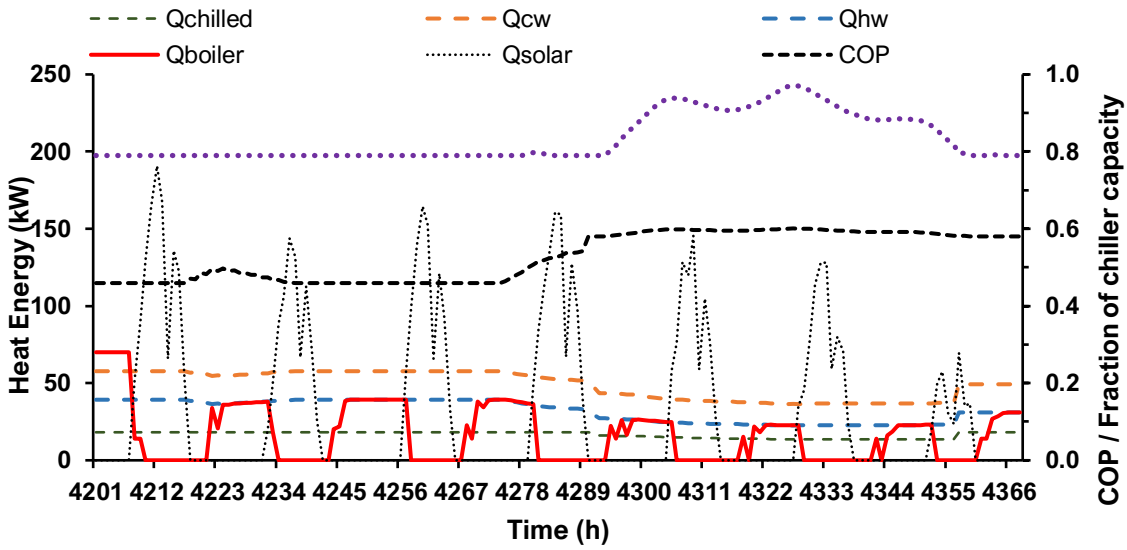

Figure 4.8: Variation of Heat transfer rates, COP and fraction of chiller capacity in a typical week of June for C1

($\dot{Q_{boiler}}$), generator ($\dot{Q_{hw}}$), condenser ($\dot{Q_{cw}}$) and evaporator ($\dot{Q_{ch}}$) are also depicted in figure 4.13 and 4.14 for C1 and C2 respectively. The results reveals that the overall values of COP, fraction of chiller nominal capacity remains the same for both configurations due to the similar values of the evaporator ($\dot{Q_{ch}}$), generator ($\dot{Q_{hw}}$) and the condenser ($\dot{Q_{cw}}$) heat flows of the chiller for both configurations. The difference only lies in the boiler energy

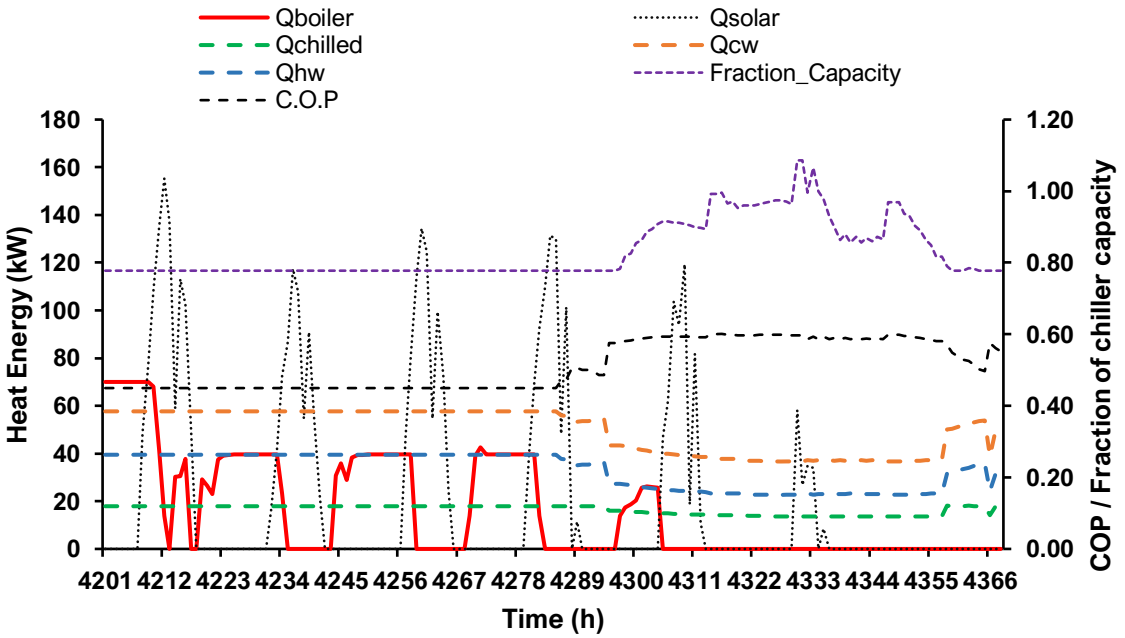

Figure 4.9: Variation of Heat transfer rates, COP and fraction of chiller capacity in a typical week of June for C2

($\dot{Q}_{boiler}$) profile. Auxiliary boiler in C1 configurations remains ON for most of the time and for the whole week, while in case of C2 the boiler remains almost OFF in the last couple of days of the week. Thereby reducing the operational cost of the system.

4.5.2 Collector Efficiency

Monthly collector efficiency for C1 and C2 are shown in the figure 4.15. The collector efficiencies presented here are for the optimum collector areas. The collector efficiencies for C1 remains in the range of 0.61-0.84 with an average yearly efficiency of 0.71. Whereas C2 it remains in the range of 0.31-0.67 with an average yearly efficiency of 0.50. the results reveal that for C1 the efficiency of the collector increases in the summer season due to the abundant available solar energy while C2 shows the efficiency trends in contrast with C1. The efficiency begins to fall once the summer season starts. The main reason for this fall in the efficiency values for the summer season is that the efficiency of the solar collector is the function of collector's inlet temperature and ambient temperature. According to Eq. 3.3 the collector's efficiency decreases as the difference between the collector's inlet temperature and the ambient temperature increases. The collector's temperature profiles of this study reveals that in C2 the average collector temperature remains elevated from the ambient temperature in the summer season which instead of absorbing heat from outside, rejects heat to the surrounding thereby decreasing the efficiency.

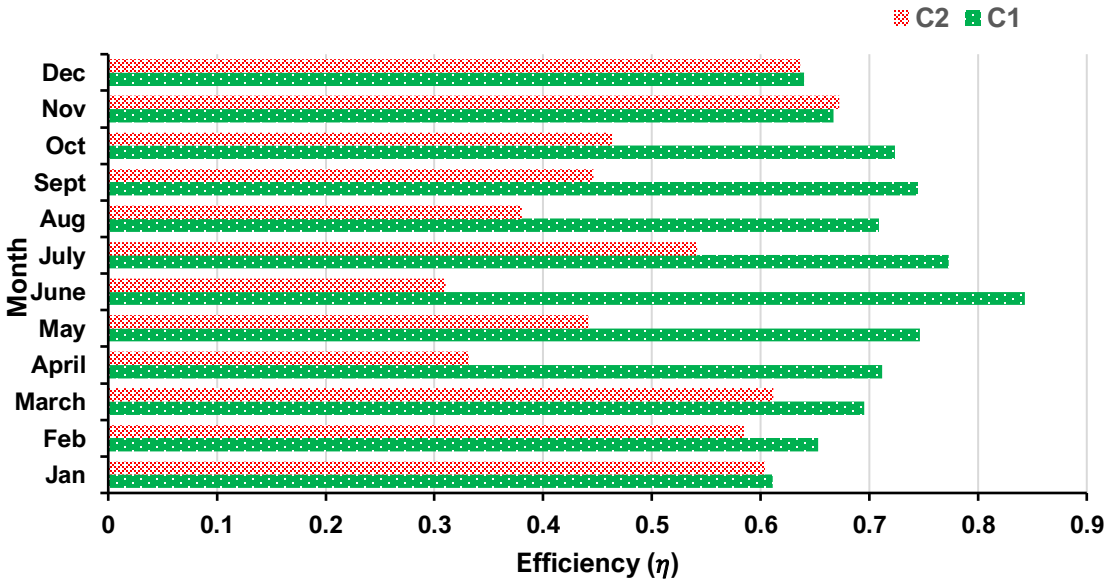

Figure 4.10: Average monthly collector efficiency for C1 and C2

4.5.3 Solar Fraction

Solar fraction is calculated to find the share of renewable energy in the total required energy by the system. The average monthly solar fractions were calculated for the optimum collector areas for both configuration models. It is evident from the figure 4.16 that C1 have more solar fraction than C2. The results show that the solar fraction for C1 lies in the range of 0.08-0.35 with an average value of 0.22. the solar fraction of C2 model is found to be in the range of 0.08-0.16 with an average value of 0.13.

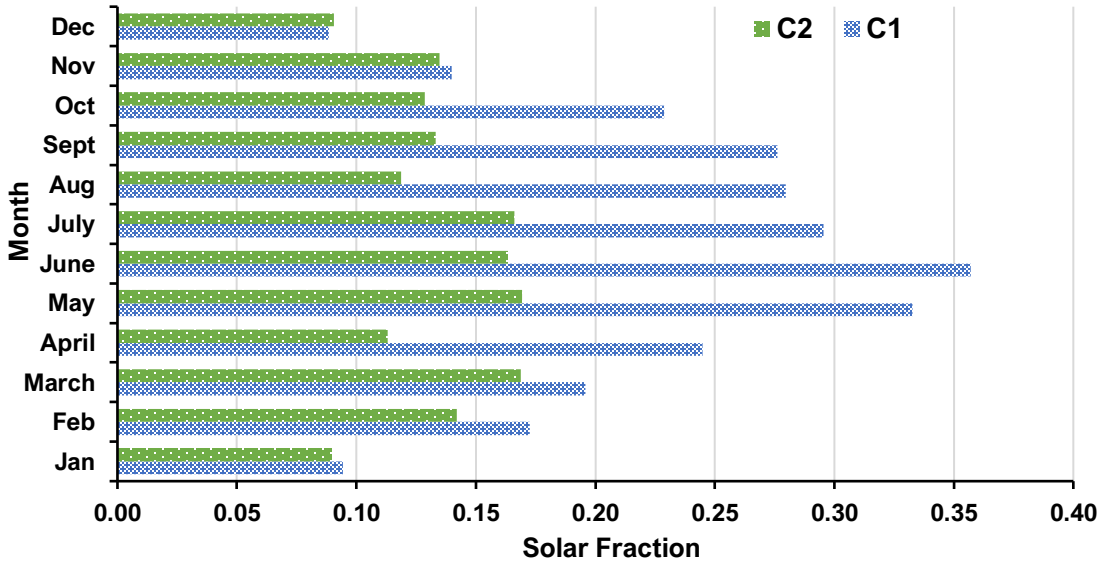

Figure 4:11: Average monthly solar fraction for C1 and C2

4.5.4 Storage Tank Temperature

Figure 4.17 shows the average monthly storage tank temperature for both configurations. The figure clearly illustrates that for C1 optimum model, the average storage tank temperature remains below the minimum temperature required by the hot water absorption chiller hence, energy from the boiler is required for the whole year to meet the chiller's operating criteria whereas, the average storage tank temperature of C2 model remains elevated from the threshold temperature required by the chiller the whole year except for the month of January and February. This is because, in C2 the fluid in the solar loop keeps circulating most of the time until the temperature returning from the chiller drops to the threshold point.

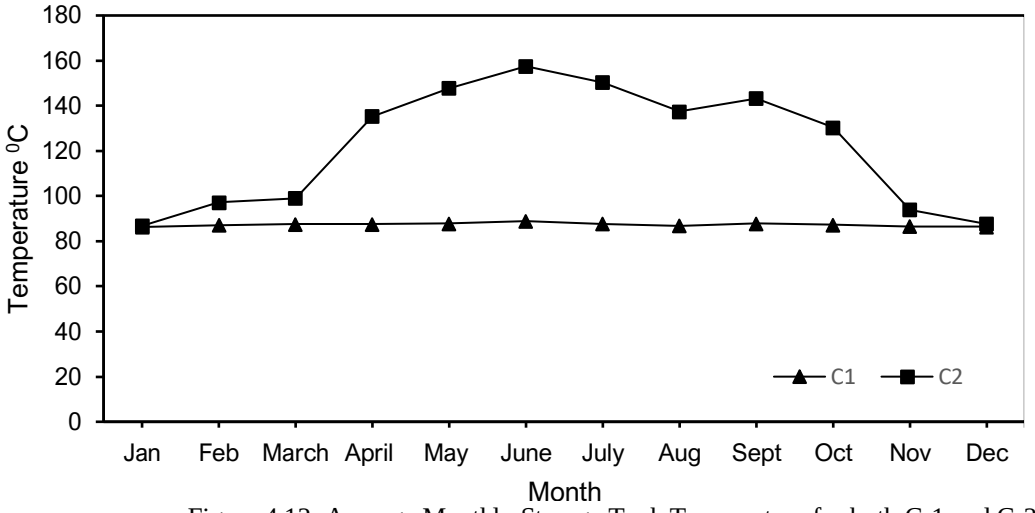

Figure 4.12: Average Monthly Storage Tank Temperature for both C-1 and C-2

4.5.5 Energy Losses from the Storage Tank:

Figure 4.18 illustrates the average monthly losses from the stratified storage tank. It is evident from the figure that the heat lost from the tank is proportional to the average tank temperature. The comparative analysis of both configurations shows that energy losses in C1 are smaller in magnitude and remains approximately the same for the whole year. Whereas for C2 its relatively higher in magnitudes and have a substantial increase in magnitude for the summer season due to the higher average storage tank temperature.

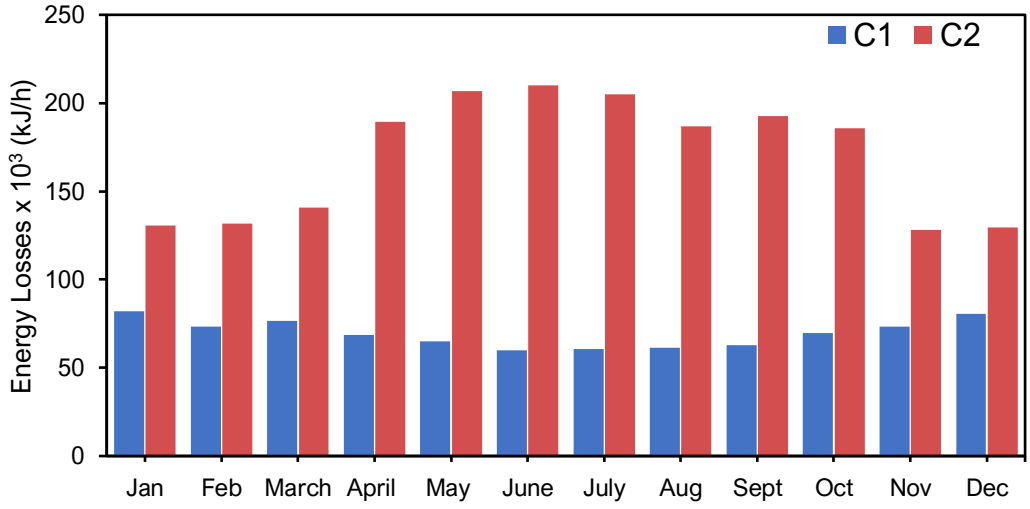

Figure 4.14: Average Monthly Heat Loss from the Storage Tank

4.5.6 Boiler Energy Input

An auxiliary boiler only gets ON when the required temperature of the working fluid is not been achieved by the solar collectors. Figure 4.19 shows the monthly average energy required by the boiler to raise the temperature of the working fluid to the required level. It is evident from the figure that C1 requires a substantial amount of boiler energy input for whole year. This large amount of energy input increases the operational cost of the system thereby, increasing the life cycle cost of the system. Whereas C2 requires nominal amount of energy in the summer, because due to the recirculation of the fluid in the solar loop the average storage tank temperature remains higher than the temperature required by the chiller. This lower energy input by the boiler reduces the operational cost and thereby the life cycle cost of the C2 model. As the energy required by the system is mostly fulfilled by the solar energy hence it reduces the combustion of natural gas in the boiler and thereby reducing the emissions of greenhouse gases from the boiler.

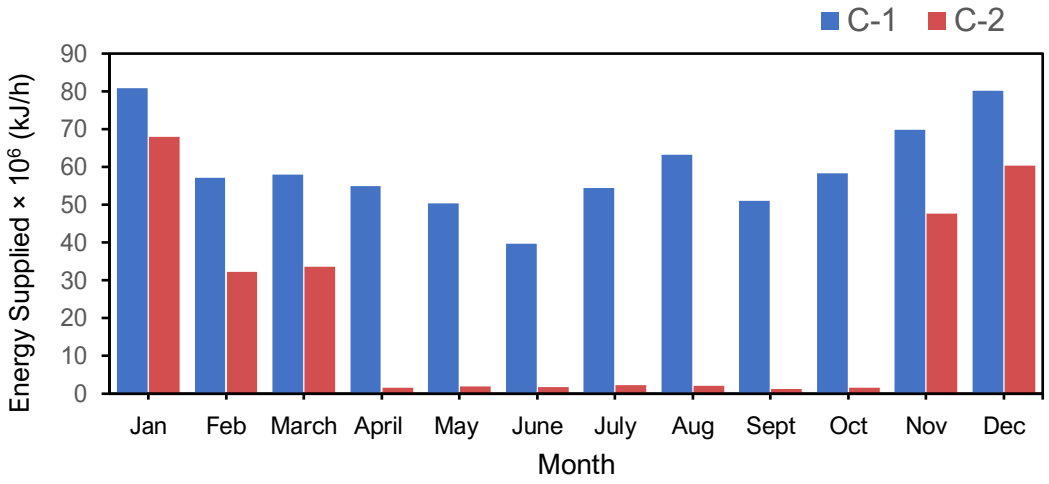

Figure 4.19: Average Monthly Energy Supplied by the Boiler

4.5.7 Economic Analysis

The economic analysis of the system is performed based on simple payback period. The simple payback period tells the number of years in which our initial cost will be recovered from savings, without considering the net present value of inflows. In the analysis both configurations were compared based on power consumption by the boiler per year and savings in PKR per year, with the base model (e.g. with no solar loop). It was found that the energy consumed by the boiler in a base model was 297576.7 kW per year with an

operational cost of 1600962 PKR per year. The initial capital cost for the optimum parameters (e.g. collector's area, storage tank volume) was 46.56 million and 39.25 million for C1 and C2, respectively. The energy savings after installing solar loop in the model was found to be 98050 kW and 226904 kW for C1 and C2, respectively. Savings in PKR at a rate of 5.38 Rs. / kWh was found to be 0.527 million and 1.22 million for C1 and C2, respectively. Figure 4.20 shows the payback period for both models and it was found that C2 has a payback period of 3.2 years as compared to C1 which have 8.8 years.

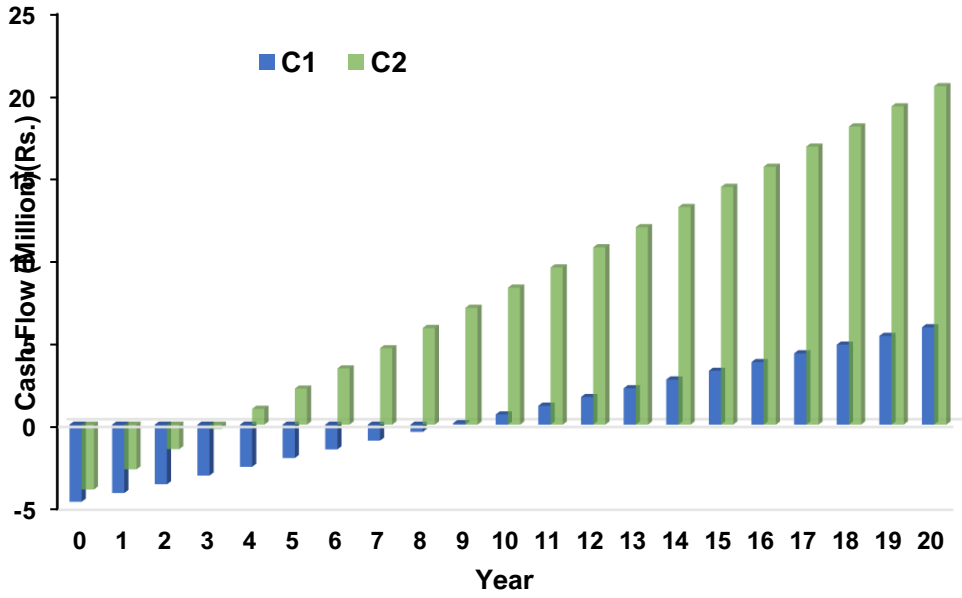

Figure 4.17: Economic analysis of C1 and C2 models

4.6 References:

[1] F. Assilzadeh, S. A. Kalogirou, Y. Ali, and K. Sopian, "Simulation and optimization of a LiBr solar absorption cooling system with evacuated tube collectors," *Renew. Energy*, vol. 30, no. 8, pp. 1143–1159, 2005, doi: 10.1016/j.renene.2004.09.017.

Chapter 5: Conclusions and Recommendations

5.1 Conclusions:

This study demonstrates the cooling of a cold storage building located in Mardan, Pakistan with a peak load of 82400 kJ/hr. (22.88 kW) through a single effect absorption chiller connected to evacuated tube solar collectors and a hot water storage tank. The cooling was achieved by modelling a SAC system in TRNSYS in two different configurations.

a) The parameters which mainly effects the Life cycle cost of a SAC system are Cost of the collector per square meter, cost of storage tank per cubic meter and cost of natural gas per kWh.
b) SAC system can be used for cold storages to achieve the required conditions throughout the year.
c) The configuration-2 having a flow diverter after the chiller is more feasible than the Configuration-1 with no flow diverter.
d) The minimum life cycle cost for C-1 and C-2 is estimated to be 28466277 PKR and 6460354 PKR, respectively.
e) The optimum collector area for C-1 and C-2 is estimated to be 150 m^2 and 120.3 m^2, respectively.
f) The optimum hot water storage tank volume for C-1 and C-2 is estimated to be 1.98 m^3 and 3.95 m^3.
g) The average hot water storage tank temperature remains higher than the chiller required temperature for the whole summer.
h) C-2 requires a very nominal amount of boiler energy in the summer season.
i) Because of the lesser boiler energy input, C-2 is considered to have less greenhouse gases emission to the environment

5.2 Future Work Suggestions:

a) The system can be revised to be used for heating processes in the storage facilities.

b) The number of hot water storage can be increased to more than one. It might have a positive impact on the overall system performance.

c) A cold-water storage tank can also be used for storing the cold water for off peak hours.

d) SAC can be modelled for different cold storage having different condition space requirement (e.g. Egg storages need 4 ^{0}C temperature).

e) The performance of the system may be assessed by using fluid other than water.

f) Use of nanofluids in the solar collector might increase the specific heat capacity of the fluid and it might have good effect on the energy capture from the collector.

g) Double and triple effect absorption can also be studied to meet the cooling load requirements.

Appendix 1

Modelling and Optimization of Solar absorption Cooling system for Cold Storages in Pakistan

Musannif Shah[1], Adeel javed[2], Hamid Ikram[3]

1. US-Pakistan Centre for Advance Studies in Energy, National University of Science and Technology (NUST) Islamabad, Pakistan, shah.musannif3@gmail.com

Abstract:

Cold storages are widely practiced methods for bulk handling of perishable fruits and vegetables. Conventional Cold storages are considered major consumer of electricity. Generally, vapor compression cooling systems are installed to achieve the required cooling conditions in conventional cold storages. Due to the energy crisis and load shedding in Pakistan, cold storages are not able to provide the required cooling in time to the food items. Solar energy can be efficiently used to fulfill the cooling requirements of the cold storages, while using the thermal operated cooling systems. The aim of this research is to model solar absorption cooling system for banana cold storage located at Peshawar for required temperature of 15 ^{0}C using dynamic modelling tool TRNSYS. Furthermore, several energy conservation measures have been simulated for cold storage building design (building envelop, insulations etc.) to explore developments in reducing cooling load and power consumption. Results revealed that actual cold storage with an operating time of 9 hours a day has maximum cooling load of 69270 kJ/h which reduced to 65200 kJ/h after applying energy conservation measures. A simulation model that contains Evacuated tube collectors (ETC), storage tank, absorption chiller and building was developed. Results depict that absorption system of rated capacity 60,000 kJ/h is required to achieve the required storage conditions. The study also reveals that to increase reliability of the system, an optimized model containing 35 m^2 collector area, hot water storage tank of 1.5 m^3 volume is required to provide effective cooling.

Key words: Cold Storage; Absorption cooling system; Solar collectors

1. Introduction

Increased energy demand and depleting fossil fuels has led to reduced natural resources. Extensive use of fossil fuels which releases greenhouse gases has adverse effect on environment[1]. Refrigeration is an energy consuming process and is responsible for approximately 1% of global GHG emissions. Cold storage consists of small stores having area 10-20 m^3 to large warehouses containing thousands of cubic meters. It contributes as a major electrical consumer in the commercial building sector. On average, the refrigerated facilities consume about 25 KWh of electricity and 9200 Btu/ft^2 per year. The function of the cold storage is to maintain the exact temperature for the storing product and to preserve the food quality[2]. A study conducted by foster showed that the specific energy consumption for chilled storages is 55.8 KWh/m^3 per year, and for frozen storages is 69.4 KWh/m^3 per year[3]. An investigation on multi floor large scale refrigerated warehouses was carried out in China and a rough estimate of the specific energy consumption of 73-91.3 KWh/m3 per year was calculated[4].

The refrigeration system needs to be designed as to provide the maximum refrigeration requirement. Mainly, the peak demands occur in few hours of the year otherwise the systems operate at the lower capacities [5]. Designing a refrigeration system for a building based on maximum cooling load results in increasing initial cost of the system[6]

The refrigeration system is based on two cycles, vapor compression and vapor absorption. Vapor compression is widely used system and is known as conventional systems. It has higher COPs, lesser weights and smaller sizes than the other systems. The major disadvantage is the utilization of CFCs and HCFCs in the vapor compression cycle, thus release of harmful refrigerants to the environment and causing the depletion of ozone layer.[7], [8]. On the other hand, the absorption system uses clean, free and renewable solar energy as an alternate to reduce

the electrical demand and to meet the cooling load of a building.[9], [10]. Besides, the working fluid for the absorption systems are water, methanol etc. which are environmentally friendly and have no or less impact on the depletion of ozone layers.[8]

In this study advance renewable energy software TRNSYS 17 is used to develop a simulation model of SAC system, which is being used by researchers around the world to study new energy concepts in renewable energy.

There had been a detailed theoretical and experimental studies on solar absorption air conditioning. A detail modelling and simulation of a solar absorption cooling system (SAC) for Abu Dhabi was been done by Islam[11]. A simulation base study using TRNSYS software was done by Balghouthi to select and optimize different components of a Solar Absorption Cooling system for Tunisia conditions[12]. A simulation and optimization analysis of a LiBr/H_2O SAC system was done by Assilzadeh. In the study Evacuated tube collectors (ETC) were used to heat water. It was concluded that to get uninterrupted operation and to improve reliability of operation of system, a hot water storage tank of 0.8 m^3 is necessary. For climate conditions of Malaysia an optimum system of 3.5 kW requires solar collectors of area 35 m^2.[13]. Florides modeled and optimized a SAC system for residential buildings for Cyprus using TRNSYS[14].

2 Research Methodology

The steps followed for modelling and simulation of solar cooling system for cold storages are shown in Fig. 1. Following is the detail description of each step.

1. Existed cold storage building was modeled in TRNSYS supported Sketchup (Google Sketchup) as shown in Fig. 2.
2. Weather data for location was imported from TRNSYS library as TMY file. Weather file consists of annual solar beam and diffused radiations, ambient dry bulb and wet bulb temperature, relative humidity and wind velocity.
3. The maximum cooling load demand is calculated for existing cold storage building to estimate the size of cooling system.
4. Energy conservation measures are applied to investigate reduction in maximum cooling load demand of building. Energy conservation measures consists of increasing insulation thickness and applying steel cladding for thermal insulation.
5. Selection of suitable components from TRNSYS library to model a solar cooling system.

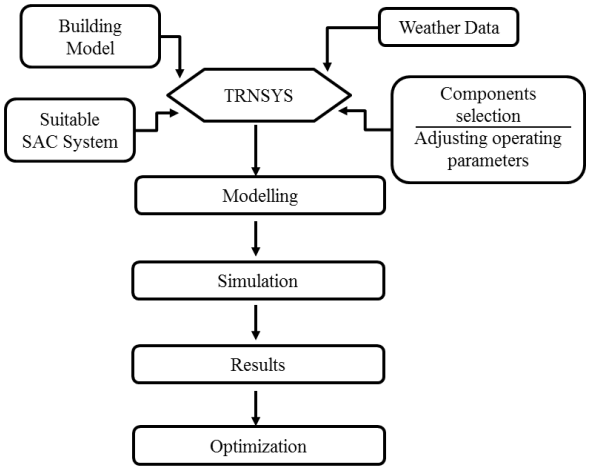

Figure 32: Technical approach of the study

6. Optimization of system components to avoid oversizing of components and reduce initial cost of the system.

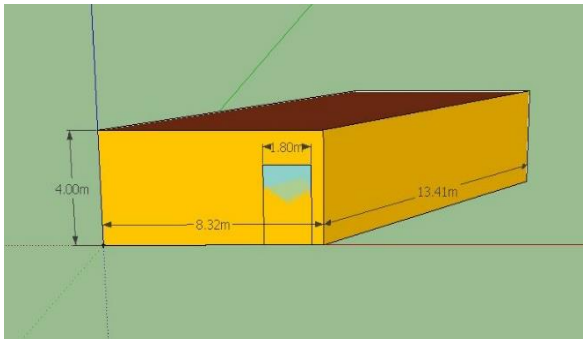

Figure 33: TRNSYS model of cold storage building

2.1 System Description

Complete Solar assisted absorption cooling system model is shown in Fig. 3. Solar absorption cooling complete model consist of 3 loops: hot water loop, cooling water loop and chilled water loop.

Hot water loop: It consists of ETC which receives solar energy from sunlight. The fluid in this loop is water which absorbs energy from the collector which results in rising its temperature. The hot water from the collectors goes into thermally insulated stratified hot

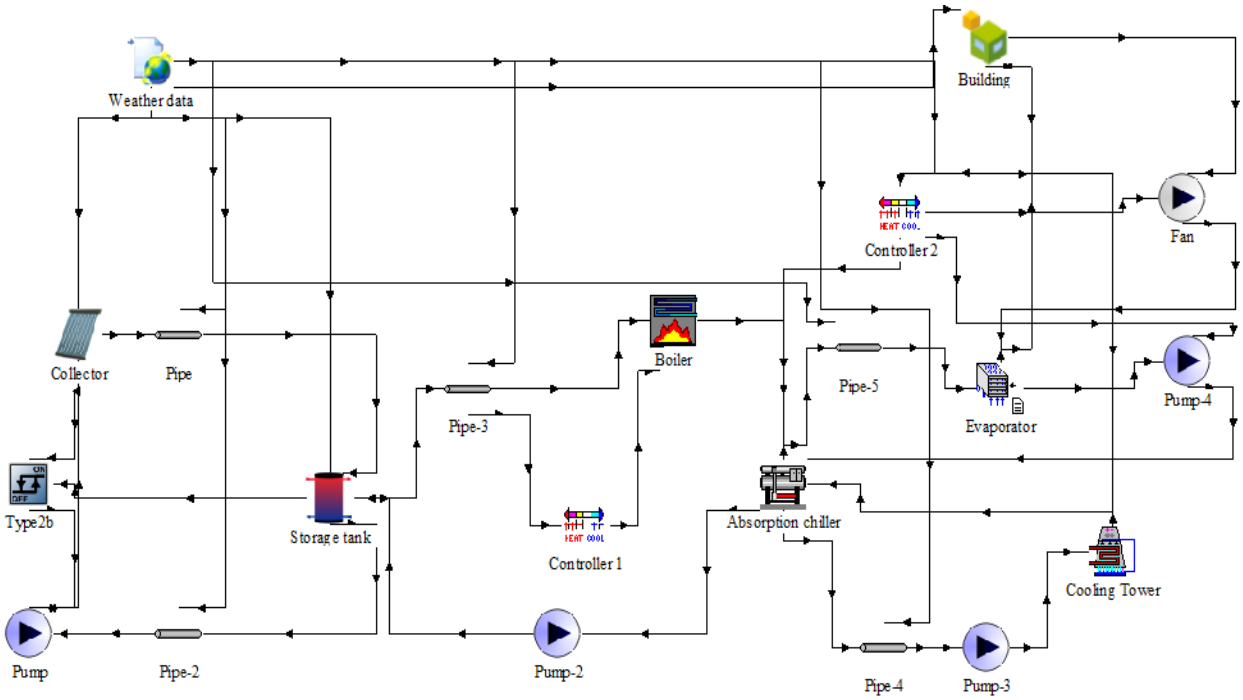

5. Figure 34: Model of SAC system in TRNSYS studio

water storage tank and then circulates back to collectors via constant speed pump. Stratified storage tank is used to increase the reliability of the system and continuous supply of hot water. The hot water from the storage tank then passes through boiler which works as auxiliary heater. It only heats water when it is below its set point temperature. After passing this hot water from generator of absorption chiller it returns to storage tank completing hot water loop.

Cooling water loop: It consists of a closed circuit cooling tower and pump. The cooling water which circulates in this loop removes heat from absorber and condenser (Q_a and Q_c) and rejects it to the atmosphere as shown in the Fig.

Chilled water loop: It consists of an evaporator, pump, fan and a thermostat controller. Chilled water from absorption chiller enters cooling coil where it absorbs heat from conditioned space and returns back to chiller via pump as shown in Fig. Thermostat gives control signal to single speed fan which circulates air from conditioned space through cooling coil.

Following is the mathematical description of important components of SAC system.

2.2 *Evacuated tube collector*

A TRNSYS Type 71 ETC is used in modeling the system. The efficiency of an ETC can be determined by Eq. 1.

$$\eta = a_0 - a_1 \frac{(\Delta T)}{I_T} - a_2 \frac{(\Delta T)^2}{I_T} \qquad (1)$$

where, a_0 is collector optimal efficiency, a_1 and a_2 are first and second order heat loss coefficients. ΔT is equal to $(T_i - T_a)$, which is difference between inlet temperature of working fluid and the ambient temperature respectively, and I_T is the incident radiations on collector aperture.

Table 1: Parameters of collectors

rameter	escription	lue
)llector pe	vacuated tube collector	
C_p	ecific heat of fluid J/kg K)	4.19
′H	ficiency mood	(T_i-T_{amb})
m_{test}	ow rate at tested ndition (kg/hr m^2)	3
a_0	tercept efficiency	0.7
a_1	ficiency slope (kJ/hr ^{2} K)	10
a_2	ficiency Curvature J/hr m^2 K^2)	0.03

The thermal efficiency of collector is defined by parameters a_0, a_1 and a_2 values of these parameters are given in Table. 1.

2.3 Absorption chiller

A hot water fired single effect, LiBr-H_2O absorption chiller (Type 107) is used in modelling of system.

The performance indices are calculated as follow:

The coefficient of performance (COP) of absorption cooling system is given in Eq. 2.

$$COP = \frac{Q_{chw}}{Q_{hw} + Q_{aux}} \quad (2)$$

Where, Q_{chw} is the energy removed from chilled water stream, Q_{hw} is the energy removed from hot water stream and Q_{aux} is the energy consumed by various electrical components such as pumps. The COP of single effect absorption chiller ranges between 0.5–0.8 and for double effect absorption chiller it ranges between 1.1–1.4[15]. Most of researches uses single effect absorption chillers due to their low initial, operation and maintenance cost[16].

The solar fraction (SF) is the fraction of cooling load that is met by solar energy. It can be calculated by Eq.3.

$$SF = \frac{Q_{coll}}{Q_{coll} + Q_{aux\ heat}} \quad (3)$$

Where: Q_{coll} is the energy delivered to hot water stream by solar collector array and $Q_{aux\ heat}$ is the energy delivered to hot water stream from auxiliary heater boiler.

2.4 Actual Building Description

The selected cold storage is located in Peshawar, Pakistan. Building has a floor area of 111.57 m^2 and four external walls of height 4 m. It has a single door on south side wall of building with an area of 4.5 m^2. The walls of cold storage building are made of 0.200 m thick common bricks layer with 0.012 plaster layer on the inner side. Roof is made of 0.10 m thick heavy weight concrete along with a layer of 0.10 m common bricks. The walls and roof are thermally insulated with polystyrene material of thickness 0.025 m. The floor is made of 0.130 m heavy weight concrete.

2.5 Modification in the Building

In the modification of building the thickness of insulation material was increased to 0.051 m and a thin sheet of steel of thickness 0.005 m was used for cladding the inside walls and roof of building.

2.6 Heat gains

Building cooling load was based on building envelop and internal heat gains. Gains were set according to ISO7730 standard with 8 persons, heavy work and lifting (470W), artificial lightning with a heat gain of 10 W/m^2 and a miscellaneous radiative power load of banana (178266 kJ/hr) with a schedule of 8 am to 5 pm daily.

2.7 Initial Component sizing

To obtain a base line for simulation, initial sizing of system components was done as shown in Table. 2. To reduce the initial cost of installation, sizing of chiller is done about 5% less than the maximum cooling demand because maximum load only occurs for one day in whole year and for the rest of year it operates on part load.[5]

Table 2: Initial component sizing

Component	Size
Absorption chiller	60000 kJ/hr
Solar collector area	35 m^2
Hot water Storage tank	m^3
Slope of Collector	30^0

3 Results and Discussions

Fig. 4. shows monthly average ambient temperature and percentage relative humidity for Peshawar, Pakistan. it is evident from the figure that ambient temperature is maximum in the month of June whereas, percent relative humidity is minimum in this month. Fig. 5. shows monthly radiation data for Peshawar including both beam and diffuse radiations. It is evident that total solar radiations are maximum in May and June having values of 1043 kJ/hr m^2 and 1089 kJ/hr m^2 respectively. It shows the potential of renewable solar energy available when cooling requirements are maximum.

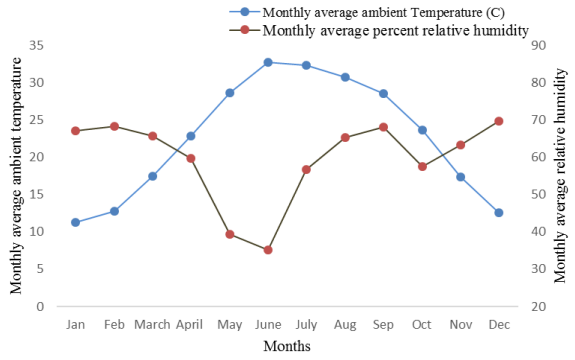

Figure 35: Monthly average ambient temperature and percentage relative humidity for Peshawar

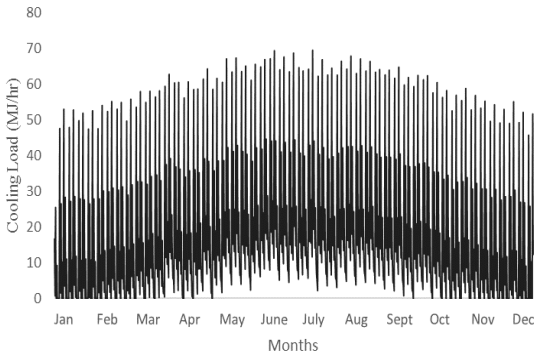

Figure 37: Hourly cooling load for actual building

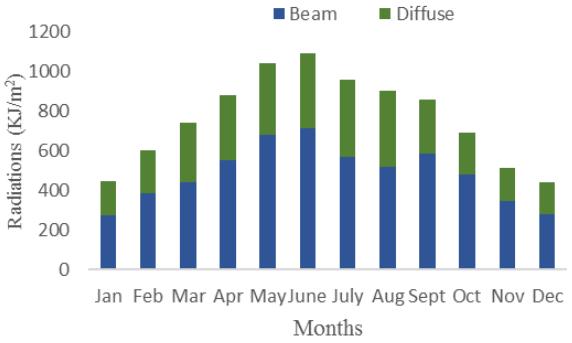

Figure 36: Average monthly beam and diffuse radiations for Peshawar

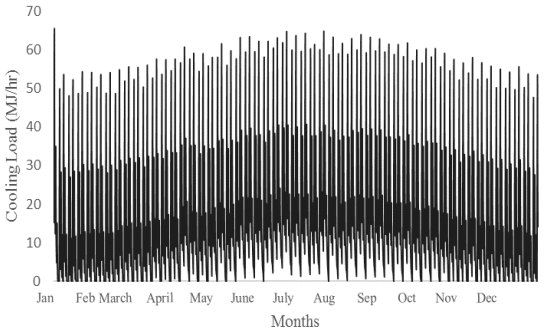

Figure 38: hourly cooling load for modified building

Hourly cooling load demand of actual building and modified building was calculated by maintaining storage temperature at 15 ^{0}C as shown in Fig. 6. and Fig. 7. respectively. Calculating maximum cooling load is essential for estimation of the size of SAC system. Investigating the figures reveals that maximum cooling load demand of actual building occurs in the month of July which is about 69270 kJ/hr. After applying the energy conservation measures there was 5.87% decrease in cooling load. The maximum cooling load demand of modified building reduces to 65200 kJ/hr. Fig. 8. shows a comparison of monthly average cooling load of existing and modified building. It is evident that there is an enormous decrease in cooling load demand for summer.

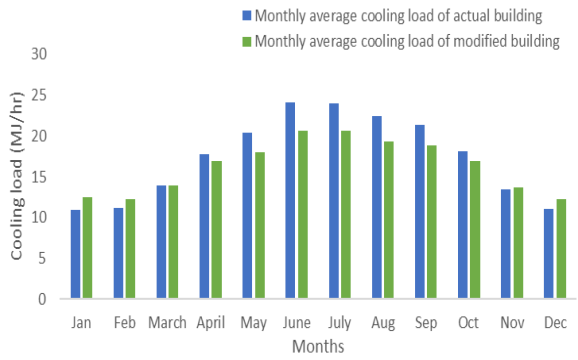

Figure 39: Monthly average cooling load of actual and modified building

3.1 Optimization of the system Components

The system optimization was done to determine Solar collector area and hot water storage tank volume at which the system achieves a highest yearly solar fraction without oversizing to minimize capital cost of the system. For this purpose, system component simulation model was run several times to get required results. Fig. 9. shows annual solar heat gain as a function of storage tank volume. As seen from the figure by increasing tank volume from 0.5 m^3 to 5 m^3 the solar heat gain first begins to increase and reaches a maximum value of 2694 MJ at tank volume of 1.5 m^3. By further increasing volume, solar heat gain reduces therefore it is appropriate to use 1.5 m^3 volume storage tank.

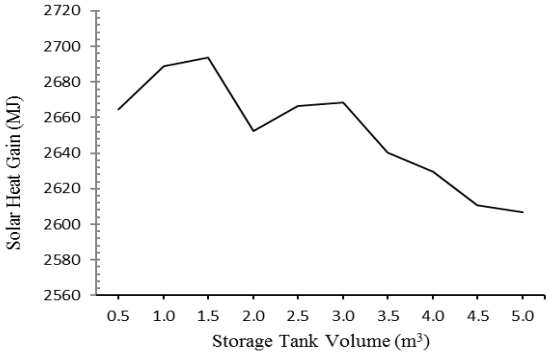

Figure 40: Effect of volume of storage tank on solar heat gain

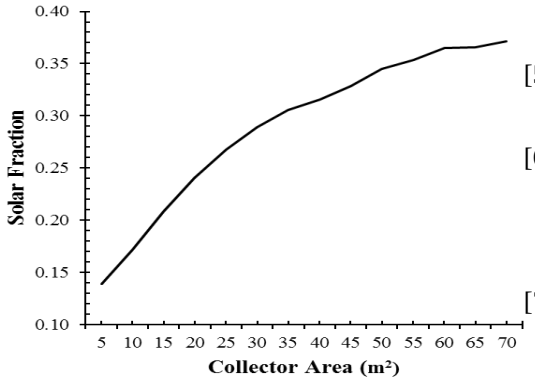

Figure 41: Variation of solar fraction with collector area

Fig.10. shows variation of solar fraction with collector area. As the collector area increases solar fraction also increases upto 35 m^2. But if we further increase area, the slop of graph gets decreasing and rise in the solar fraction is comparatively less therefore the optimize solar collector area is 35 m^2

4. Conclusion

Modelling and optimization of solar assisted absorption cooling system for a cold storage in Peshawar, Pakistan has been carried out. Results from simulations reveals that after applying modification and energy conservation measures to cold storage building the maximum cooling load reduced from 69270 kJ/h to 65200kJ/h. The optimization analysis conducted for the system sizing reveals that an evacuated tube collector array of 35 m^2 area and 1.5 m^3 hot water storage tank are appropriate to use so that to minimize the initial cost and increase the reliability of the system.

5. References:

] K. P. Amber, R. Ahmad, M. W. Aslam, A. Kousar, M. Usman, and M. S. Khan, "Intelligent techniques for forecasting electricity consumption of buildings," *Energy*, vol. 157, pp. 886–893, 2018.

] J. A. Evans *et al.*, "Specific energy consumption values for various refrigerated food cold stores," *Energy Build.*, vol. 74, no. 2014, pp. 141–151, 2020.

[3] J. A. Evans *et al.*, "Assessment of methods to reduce the energy consumption of food cold stores," *Appl. Therm. Eng.*, vol. 62, no. 2, pp. 697–705, 2014.

[4] F. Tian, "An agri-food supply chain traceability system for China based on RFID & blockchain technology," *2016 13th Int. Conf. Serv. Syst. Serv. Manag. ICSSSM 2016*, 2016.

[5] K. Street and L. E. Gb, "Ep 1 492 748 b1 (12)," vol. 1, no. 19, pp. 1–10, 2010.

[6] H. Chen, T. Ngoc, W. Yang, C. Tan, and Y. Li, "Progress in electrical energy storage system : A critical review," *Prog. Nat. Sci.*, vol. 19, no. 3, pp. 291–312, 2009.

[7] J. P. Praene, O. Marc, F. Lucas, and F. Miranville, "Simulation and experimental investigation of solar absorption cooling system in Reunion Island," *Appl. Energy*, vol. 88, no. 3, pp. 831–839, 2011.

[8] K. Habib, B. Choudhury, P. Kumar, and B. Baran,

"Study on a solar heat driven dual-mode adsorption chiller," *Energy*, vol. 63, pp. 133–141, 2013.

[9] C. Sanjuan, S. Soutullo, and M. R. Heras, "Optimization of a solar cooling system with interior energy storage," *Sol. Energy*, vol. 84, no. 7, pp. 1244–1254, 2010.

[10] X. Garcı, "Solar absorption cooling in Spain : Perspectives and outcomes from the simulation of recent installations ´ a Casals *," vol. 31, pp. 1371–1389, 2006.

[11] A. Al-Alili, M. D. Islam, I. Kubo, Y. Hwang, and R. Radermacher, "Modeling of a solar powered absorption cycle for Abu Dhabi," *Appl. Energy*, vol. 93, pp. 160–167, 2012.

[12] M. Balghouthi, M. H. Chahbani, and A. Guizani, "Feasibility of solar absorption air conditioning in Tunisia," *Build. Environ.*, vol. 43, no. 9, pp. 1459–1470, 2008.

[13] F. Assilzadeh, S. A. Kalogirou, Y. Ali, and K. Sopian, "Simulation and optimization of a LiBr solar absorption cooling system with evacuated tube collectors," *Renew. Energy*, vol. 30, no. 8, pp. 1143–1159, 2005.

[14] G. A. Florides, S. A. Kalogirou, S. A. Tassou, and L. C. Wrobel, "Modelling, simulation and warming impact assessment of a domestic-size absorption solar cooling system," *Appl. Therm. Eng.*, vol. 22, no. 12, pp. 1313–1325, 2002.

[15] U. Eicker and D. Pietruschka, "Design and performance of solar powered absorption cooling systems in office buildings," vol. 41, pp. 81–91, 2009.

[16] Y. Hang, L. Du, M. Qu, and S. Peeta, "Multi-objective optimization of integrated solar absorption cooling and heating systems for medium-sized of fi ce buildings," *Renew. Energy*, vol. 52, pp. 67–78, 2013.